Biomechanics and Modeling in Mechanobiology manuscript No.
(will be inserted by the editor)

Invariant Theory for Dispersed Transverse Isotropy

An Efficient Means for Modeling Fiber Splay

Alan D. Freed[1], Daniel R. Einstein[2], Ivan Vesely[2]

[1] Polymers Branch, Materials Division, MS 49-3
NASA's John H. Glenn Research Center at Lewis Field
21000 Brookpark Road
Brook Park, OH 44135, USA.
And: Department of Biomedical Engineering, ND-20
The Cleveland Clinic Foundation
9500 Euclid Avenue
Cleveland, OH 44195, USA. e-mail: Alan.D.Freed@nasa.gov

[2] Cardiothoracic Surgery Research
Saban Research Institute, MS 66
Children's Hospital Los Angeles
4650 Sunset Boulevard
Los Angeles, CA 90027, USA. e-mail: IVesely@chla.usc.edu

Received: 28 April 2004 / Revised version: date

Abstract Most soft tissues possess an oriented architecture of collagen fiber bundles, conferring both anisotropy and nonlinearity to their elastic behavior. Transverse isotropy has often been assumed for a subset of these tissues that have a single macroscopically-identifiable preferred fiber direction. Micro-structural studies, however, suggest that, in some tissues, collagen fibers are approximately normally distributed about a mean preferred fiber direction. Structural constitutive equations that account for this dispersion of fibers have been shown to capture the mechanical complexity of these tissues quite well. Such descriptions, however, are computationally cumbersome for two-dimensional (2D) fiber distributions, let alone for fully three-dimensional (3D) fiber populations. In this paper, we develop a new constitutive law for such tissues, based on a novel invariant theory for dispersed transverse isotropy. The invariant theory is based on a novel closed-form 'splay invariant' that can easily handle 3D fiber populations, and that only requires a single parameter in the 2D case. The model is polyconvex and fits biaxial data for aor-

* Research partially funded by the US DOD via Award No. DAMD17-01-1-0673 to the Cleveland Clinic Foundation and Children's Hospital Los Angeles.
Send offprint requests to: Alan D. Freed
Correspondence to: Alan D. Freed

tic valve tissue as accurately as the standard structural model. Modification of the fiber stress-strain law requires no re-formulation of the constitutive tangent matrix, making the model flexible for different types of soft tissues. Most importantly, the model is computationally expedient in a finite-element analysis.

Key words nonlinear elasticity – invariant theory – anisotropy

1 Introduction

Constitutive modeling of soft tissues is an important prerequisite for the computational analysis of the systems-level response of biological structures to applied loads and pressures. Computational modeling in many cases is the only way, short of implantation, to evaluate the mechanical response of tissues to the full 3D mechanical environment seen *in vivo*. Moreover, computational modeling permits the analyst to directly query the relationship between structure and stress, and to explore the design space of newly proposed, implants, bioprostheses or tissue-engineered constructs. Numerical models of tissue systems can be computationally intensive. This is particularly true of tissues that require complex material models, and systems that involve fluid-structure interactions. The material models used in these systems must not only be accurate, they must also be computationally efficient.

The past few years have seen an increased interest in nonlinear continuum mechanics as a framework for describing the mechanical behavior of soft tissues. The now well-established mathematics of this field provides a perspective from which rigorous, thermodynamically-reasonable constitutive equations can be proposed—a characteristic that was lacking in many earlier *ad hoc* tissue descriptions. The geometric and material nonlinearities seen in tissues fit well into this framework, and anisotropy is readily handled by the theory of invariants [Spencer, 1972]. In addition, constitutive equations posed within this framework can call upon developed computational techniques, permitting the exploration of tissue-level and organ-level mechanics involving finite deformations. An excellent reference for both nonlinear continuum mechanics and related variational principles, as they apply to soft tissues, is the textbook by [Holzapfel, 2000]

Structural constitutive equations that view soft tissues as statistically-oriented distributions of fibers come from a different tradition based on the experimental observation of fiber dispersion, or splay. For example, [Sacks, 2003] showed a correlation between the intensity distribution of the small-angle light scattering of bovine pericardium and both fiber orientation and dispersion. Similarly, [Holzapfel et al., 2002] showed that smooth muscle cells in arterial media are statistically oriented around two opposing helical directions. From these cellular orientations, collagen fiber orientations were inferred. An earlier observation of fiber dispersal in bovine pericardium was documented by [Zioupos and Barbenel, 1994]. The need to account for fiber dispersion architectures when modeling soft tissues was first addressed by [Lanir, 1983]. Since then, structural models with dispersion have been proposed for passive myocardium [Horowitz et al., 1988], lung

[Mijailovich et al., 1993], heart valves [Sacks, 2000], aorta [Wuyts et al., 1995], and tendon and ligament [Hurschler et al., 1997]. To model fiber splay, typically either a von Mises [Hurschler et al., 1997] or Gaussian [Sacks, 2000] distribution is adopted.

Mathematically, the inclusion of such probability distribution functions into constitutive models presents little challenge, but computationally, they are cumbersome. The probability density function acts as a weighting function for a fiber stress-strain rule. Functionally, in the 2D case, this can be represented as

$$\mathbf{S} = \int_{-\pi/2}^{\pi/2} S_f(\theta)\, R(\theta)\, \mathbf{N}(\theta) \otimes \mathbf{N}(\theta)\, \mathrm{d}\theta, \tag{1}$$

where $\mathbf{S}$ is the second Piola-Kirchhoff stress, $S_f(\theta)$ is a fiber stress-strain rule, $R(\theta)$ is a probability distribution function, and $\mathbf{N}(\theta) \otimes \mathbf{N}(\theta)$ governs the orientation of a fiber family in the 2D plane. What is important to note is that the product of fiber stress and the weighting function must be integrated over a full semicircle in the 2D case, Eq. (1), or an equivalent hemisphere in the 3D case. These integrals have traditionally been evaluated numerically. Numerical experiments on one such equation for mitral-valve tissue suggested that eighteen discrete intervals were necessary to capture the full range of constitutive behavior [Einstein, 2002]. This is mechanically equivalent to having eighteen weighted fibers in the plane. A single integral of this kind in the constitutive equation implies two integrals to be evaluated in the constitutive tangent matrix. Likewise, 3D fiber dispersion would require two integrals to be evaluated for stress, and four for the constitutive tangent matrix. In the computational model, these operations are evaluated at every iteration, of every time step, at every Gauss point, for every finite element, in some geometric model of interest.

In this paper, we develop an alternative constitutive law for tissues whose collagen fiber populations are statistically distributed. To address the problem of computational cost, the integral in Eq. (1) is replaced with a novel closed-form 'splay invariant' that requires a single parameter in the 2D case, and a single operation per iteration. To evaluate the model, we compare its correlative capability against biaxial data for aortic-valve tissue. In addition, we compare the capabilities of our model against those of a published structural model [Billiar and Sacks, 2000b, Einstein, 2002] that is based on the paradigm in Eq. (1) and which fits the data quite well.

2 Theory

Consider a mass point originally given by the set of coordinates $\mathbf{X} = (X_1, X_2, X_3)$ assigned at an arbitrary reference time of t_0. At current time t, this mass element is located by a different set of coordinates $\mathbf{x} = (x_1, x_2, x_3)$. Let the motion of this mass point through space be described by a one-parameter family (in time) of locations considered to be continuous and sufficiently differentiable to allow the definition

of a deformation gradient

$$F_{ij}(t_0,t)=\frac{\partial x_i}{\partial X_j},\quad \text{or in tensor notation,}\quad \mathsf{F}(t_0,t)=[\![\partial x_r/\partial X_c]\!], \tag{2}$$

where indices r and c denote row and column, and have values 1, 2, 3. The ability to invert this field (i.e., $\mathsf{F}^{-1}(t_0,t)=[\![\partial X_r/\partial x_c]\!]$ such that $\mathsf{F}^{-1}\mathsf{F}=\mathsf{F}\mathsf{F}^{-1}=\mathsf{I}$, where $\mathsf{I}=[\![\delta_{rc}]\!]$ is the identity tensor and δ_{ij} denotes the Kronecker delta) ensures that a given particle cannot occupy two locations at the same instant in time, and that two discrete particles cannot occupy a single location at any given moment in time.

Affiliated with the deformation gradient defined in Eq. (2) are the left- and right-deformation tensors[1] defined by

$$\mathsf{B}=\mathsf{F}\mathsf{F}^{\mathrm{T}}\quad\text{and}\quad\mathsf{C}=\mathsf{F}^{\mathrm{T}}\mathsf{F}, \tag{3}$$

respectively, where '$^{\mathrm{T}}$' implies matrix transpose (e.g., $\mathsf{B}(\mathbf{x};t_0,t)=[\![F_{rk}F_{ck}]\!]$ and $\mathsf{C}(\mathbf{X};t_0,t)=[\![F_{kr}F_{kc}]\!]$ with the repeated index k being summed from 1 to 3 in the usual manner). Inverses B^{-1} and C^{-1} exist because the tensor fields B and C are symmetric positive-definite. The left-deformation tensor B appears in Eulerian constructions, while the right-deformation tensor C appears in Lagrangian constructions.

2.1 Invariants

Consider a vector $\mathbf{a}_0=[\![a_r(\mathbf{X};t_0)]\!]$ of length $\mathbf{a}_0\cdot\mathbf{a}_0=a_k(\mathbf{X};t_0)\,a_k(\mathbf{X};t_0)=1$ that lies tangent to a material line of strength (e.g., a fiber) in the reference state t_0. After a deformation, this material line will have stretched by an amount $\lambda(t_0,t)$ that is quantified by $\lambda^2=\mathbf{a}_0\cdot\mathsf{C}\mathbf{a}_0=a_k(\mathbf{X};t_0)\,C_{k\ell}(\mathbf{X};t_0,t)\,a_\ell(\mathbf{X};t_0)$. As such, there exists a spatial vector $\mathbf{a}=[\![a_r(\mathbf{x};t)]\!]$ with $L2$ norm $\|\mathbf{a}\|_2=(\mathbf{a}\cdot\mathbf{a})^{1/2}=\lambda$ that in the deformed state t of Green's metric C relates to material vector $\mathbf{a}_0$ via the mapping $\mathbf{a}=\mathsf{F}\mathbf{a}_0$, which is the transformation law of a polar vector.[2]

From the classic theory of invariants [Spencer, 1972], there are five invariants that are needed to describe a material with transverse isotropy (i.e., a material with a single fiber family); they are:

$$I_I=\operatorname{tr}\mathsf{C},\quad I_{II}=\tfrac{1}{2}((\operatorname{tr}\mathsf{C})^2-\operatorname{tr}(\mathsf{C}^2)),\quad I_{III}=\det\mathsf{C}=(\det\mathsf{F})^2, \tag{4}$$

$$I_{IV}=\mathbf{a}_0\cdot\mathsf{C}\mathbf{a}_0=\mathbf{a}\cdot\mathbf{a}=\lambda^2,\quad I_V=\mathbf{a}_0\cdot\mathsf{C}^2\mathbf{a}_0=\mathbf{a}\cdot\mathsf{B}\mathbf{a}, \tag{5}$$

---

[1] Tensors $\mathsf{B}=\mathsf{F}\mathsf{F}^{\mathrm{T}}=\mathsf{V}^2$ and $\mathsf{C}=\mathsf{F}^{\mathrm{T}}\mathsf{F}=\mathsf{U}^2$ are often referred to as the left and right *Cauchy-Green* deformation tensors, respectively, because V and U are called the left- and right-stretch tensors, so named because of the polar decomposition $\mathsf{F}=\mathsf{V}\mathsf{R}=\mathsf{R}\mathsf{U}$ wherein $\mathsf{R}\mathsf{R}^{\mathrm{T}}=\mathsf{I}$. We prefer to call B and C the left- and right-deformation tensors. Historically, [Cauchy, 1827, pp. 60–69] used B^{-1} (sometimes expressed as c) and [Green, 1841] used C, while [Finger, 1894] introduced their duals, B (sometimes expressed as b) and C^{-1}. Therefore, naming these fields after Cauchy and Green seems an injustice to Finger, especially since Finger introduced B into the literature.

[2] The transformation law $\mathbf{b}=\mathsf{F}^{-\mathrm{T}}\mathbf{b}_0$ applies to axial vectors whose norms $\|\mathbf{b}\|_2=(\mathbf{b}\cdot\mathbf{b})^{1/2}$ are measured against Finger's metric C^{-1}. We have no need for axial vectors in this work.

where $\mathrm{tr}\,\mathbf{C} = C_{kk}$ is the trace of $\mathbf{C}$, and $\det\mathbf{C} = \frac{1}{3}\{\mathrm{tr}\,\mathbf{C}^3 - \mathrm{tr}\,\mathbf{C}[(\mathrm{tr}\,\mathbf{C})^2 - 3\,\mathrm{tr}\,\mathbf{C}^2]\}$ denotes its determinant. The three invariants in Eq. (4) account for isotropic effects, while the two invariants in Eq. (5) account for anisotropic effects.

Invariants I_N and I_V idealize all fibers in a family as being parallel, which is not indicative of soft tissues. The fiber architectures of soft tissues are splayed. We therefore seek an alternative pair of invariants—call them $I_{\langle N\rangle}$ and $I_{\langle V\rangle}$—that can replace I_N and I_V for dispersed fiber architectures, yet analytically reduce to I_N and I_V in the absence of fiber dispersion. It is sufficient to define these new invariants as

$$I_{\langle N\rangle} = \mathrm{tr}(\mathbf{FKF}^{\mathrm{T}}) = \mathrm{tr}(\mathbf{KC}) \quad \text{and} \quad I_{\langle V\rangle} = \mathrm{tr}(\mathbf{CKC}), \tag{6}$$

where $\mathbf{K}(\mathbf{X};t_0)$ is constrained such that $\mathbf{K} \rightarrow \mathbf{a}_0 \otimes \mathbf{a}_0 = [\![a_r(\mathbf{X};t_0)a_c(\mathbf{X};t_0)]\!]$ in the absence of splay. Tensor $\mathbf{K}$ is a material constant. The main objective of this paper is to derive such a $\mathbf{K}$ appropriate for describing the anisotropy caused by fiber dispersion.

2.2 *Elasticity*

The strain-energy density per unit mass, when written in the Lagrangian frame, is given by [Lodge, 1974, pp. 194–195]

$$\mathrm{d}W = \frac{1}{2\varrho_0}\,\mathrm{tr}(\mathbf{S}\,\mathrm{d}\mathbf{C}), \tag{7}$$

where $\mathrm{d}W(\mathbf{X};t_0,t,\mathrm{d}t)$ represents the work done on a material element of mass density $\varrho = \varrho(\mathbf{x};t)$, with $\varrho_0 = \varrho(\mathbf{X};t_0)$. Work is caused by an imposed displacement acting on the mass element, manifested here as the strain increment $\frac{1}{2}\mathrm{d}\mathbf{C}(\mathbf{X};t_0,t,\mathrm{d}t)$. The material responds to this displacement through the creation of forces, thereby producing a state of stress $\mathbf{S}(\mathbf{X};t_0,t)$.

The second Piola-Kirchhoff stress tensor $\mathbf{S}$ pulls forward into the Eulerian frame [Holzapfel, 2000, pp. 82–84] becoming the Cauchy stress tensor $\mathbf{T}(\mathbf{x};t)$ via the well-known mapping $\mathbf{S} = \frac{\varrho_0}{\varrho}\mathbf{F}^{-1}\mathbf{T}\mathbf{F}^{-\mathrm{T}}$. Formula $\frac{\varrho_0}{\varrho} = \det\mathbf{F}$ follows from the conservation of mass. Green strain $\mathbf{E}(\mathbf{X};t_0,t)$, defined by $\mathbf{E} = \frac{1}{2}(\mathbf{C}-\mathbf{I})$, has an incremental change $\mathrm{d}\mathbf{E}(\mathbf{X};t_0,t,\mathrm{d}t)$ of $\mathrm{d}\mathbf{E} = \frac{1}{2}\mathrm{d}\mathbf{C} = \mathbf{F}^{\mathrm{T}}\hat{\mathbf{E}}\mathbf{F}$, wherein $\hat{\mathbf{E}}(\mathbf{x};t,t{+}\mathrm{d}t) = \frac{1}{2}(\hat{\mathbf{C}}-\mathbf{I})$ with $\hat{\mathbf{C}}(\mathbf{x};t,t{+}\mathrm{d}t) = \hat{\mathbf{F}}^{\mathrm{T}}\hat{\mathbf{F}}$ given that $\hat{\mathbf{F}}(t,t{+}\mathrm{d}t) = [\![\partial x_r(t{+}\mathrm{d}t)/\partial x_c(t)]\!]$.

An elastic solid is defined by the constitutive law [Leonov, 2000]

$$\mathbf{S} = 2\varrho_0\,\frac{\partial W(T,\mathbf{C})}{\partial \mathbf{C}}, \tag{8}$$

with an isochoric constraint of $\det\mathbf{F} = 1$ also applying whenever the material is incompressible. Thermodynamics requires W to be a function of both temperature T and deformation $\mathbf{C}$. Because the human body maintains a nearly isothermal state, the temperature dependence of tissues is usually neglected in their analysis. The strain-energy density W will also depend on any number of material constants that may appear as scalar, vector, or tensor fields.

Adopting the invariants in Eqs. (4 & 6) as our integrity basis, the general constitutive equation for a transversely isotropic elastic solid with splay, when expressed in the Lagrangian frame, yields the constitutive equation[3]

$$\mathsf{S} = (\mathcal{W}_{,I} + I_I\mathcal{W}_{,II})\mathsf{I} - \mathcal{W}_{,II}\mathsf{C} + I_{III}\mathcal{W}_{,III}\mathsf{C}^{-1} + \mathcal{W}_{,\langle IV\rangle}\mathsf{K} + \mathcal{W}_{,\langle V\rangle}(\mathsf{CK} + \mathsf{KC}), \quad (9)$$

that, when pushed forward into the Eulerian frame, becomes

$$\boldsymbol{\tau} = (\mathcal{W}_{,I} + I_I\mathcal{W}_{,II})\mathsf{B} - \mathcal{W}_{,II}\mathsf{B}^2 + I_{III}\mathcal{W}_{,III}\mathsf{I} + \mathcal{W}_{,\langle IV\rangle}\mathsf{A} + \mathcal{W}_{,\langle V\rangle}(\mathsf{BA} + \mathsf{AB}), \quad (10)$$

where $\mathcal{W}_{,I} = 2\varrho_0\,\partial W/\partial I_I$, etc., and $\mathsf{A}(\mathbf{x};t_0,t) = \mathsf{FKF}^{\mathrm{T}}$. Tensor $\boldsymbol{\tau}(\mathbf{x};t_0,t) = \frac{\varrho_0}{\varrho}\mathsf{T}$ is known as the Kirchhoff stress.

It is a straightforward matter to extend any, existing, transversely isotropic, integrity basis into an equivalent basis that accounts for splay by applying an appropriate mapping. For example, the classic integrity basis $\{I_I, I_{II}, I_{III}, I_{IV}, I_V\}$ maps into the basis $\{\beta_I,\beta_{II},\beta_{III},\beta_{IV},\beta_V\}$ derived by [Criscione et al., 2001] via their formulæ (5.3 & 5.4). To introduce splay into their integrity basis, one simply applies these same mappings, but with $\{I_I, I_{II}, I_{III}, I_{\langle IV\rangle}, I_{\langle V\rangle}\}$ replacing $\{I_I, I_{II}, I_{III}, I_{IV}, I_V\}$, which produces $\{\beta_I,\beta_{\langle II\rangle},\beta_{\langle III\rangle},\beta_{\langle IV\rangle},\beta_{\langle V\rangle}\}$ as its equivalent set of splay invariants.

The challenges that lie ahead are: *i*) to establish a tensor field K which is appropriate for splayed fiber architectures, and *ii*) to arrive at a simple set of five scalar-valued gradients $\{\mathcal{W}_{,I}, \mathcal{W}_{,II}, \mathcal{W}_{,III}, \mathcal{W}_{,\langle IV\rangle}, \mathcal{W}_{,\langle V\rangle}\}$ that allows Eqs. (9 & 10) to aptly describe some known set of experimental data.

3 Anisotropic Stiffness

For purposes of assessing the effect of fiber orientation on stiffness, it is useful to switch from the global coordinate system (X, Y, Z) with base vectors $\{\mathbf{e}_X, \mathbf{e}_Y, \mathbf{e}_Z\}$ to a local or intrinsic coordinate system $(1, 2, 3)$ with base vectors $\{\mathbf{e}_1, \mathbf{e}_2, \mathbf{e}_3\}$. These local coordinates are selected so that the unit vector in the 1-direction (i.e., $\mathbf{e}_1$) is coaxial with the mean direction of fiber orientation $\mathbf{a}_0$, while the unit vectors in the 2- and 3-directions lie in the transverse plane. Because both the intrinsic and global coordinate systems are considered to be rectangular Cartesian, there exists an unique, orthogonal, rotation matrix Q such that

$$\mathbf{e}_X = \mathsf{Q}\mathbf{e}_1, \quad \mathbf{e}_Y = \mathsf{Q}\mathbf{e}_2, \quad \mathbf{e}_Z = \mathsf{Q}\mathbf{e}_3, \quad (11)$$

where $\mathsf{Q}^{\mathrm{T}}\mathsf{Q} = \mathsf{I}$ with $\det\mathsf{Q} = 1$. Matrix Q represents a rigid-body rotation.

[3] The following well-known tensor derivatives are useful in the derivation of constitutive formulæ:

$$\frac{\partial\,\mathrm{tr}\,\mathsf{Z}}{\partial\mathsf{Z}} = \mathsf{I} \quad \frac{\partial\,\mathrm{tr}\,\mathsf{Z}^{-1}}{\partial\mathsf{Z}} = -\mathsf{Z}^{-\mathrm{T}}\mathsf{Z}^{-\mathrm{T}}, \quad \frac{\partial\det\mathsf{Z}}{\partial\mathsf{Z}} = \det(\mathsf{Z})\,\mathsf{Z}^{-\mathrm{T}}.$$

3.1 Two-Dimensional Splay Invariants

For transversely isotropic 2D membranes, the unit vector $\mathbf{e}_f$ in the intrinsic coordinate frame that locates a specific fiber tangent within a given fiber distribution is described via polar coordinates

$$\mathbf{e}_f(\theta) = \cos(\theta)\,\mathbf{e}_1 + \sin(\theta)\,\mathbf{e}_2, \tag{12}$$

where angle θ orients $\mathbf{e}_f$ with respect to the mean-fiber direction $\mathbf{e}_1$ (i.e., to $\mathbf{a}_0$) in the plane of a membrane (viz., the 12 plane).

We adopt the Gaussian formulation primarily because it allows analytic solutions (cf. Apps. A & B). The cosine of the angle between the mean-fiber direction $\mathbf{e}_1$ and that of an individual fiber $\mathbf{e}_f$ is given by the inner product $\mathbf{e}_1 \cdot \mathbf{e}_f$, which from Eq. (12) is just $\cos\theta$. The Gaussian distribution governing a single fiber family (i.e., transverse isotropy), when expressed in the local coordinate system $(1, 2, 3)$ with base vectors $\{\mathbf{e}_1, \mathbf{e}_2, \mathbf{e}_3\}$, is therefore simply

$$\frac{1}{\alpha\sqrt{2\pi}}\exp\left(\frac{-\theta^2}{2\alpha^2}\right),$$

with α being a standard deviation in the angle of fiber dispersion about the mean-fiber direction $\mathbf{e}_1$. Because the local coordinate direction $\mathbf{e}_1$ is coincident with the mean-fiber direction $\mathbf{a}_0$, there is no angle between $\mathbf{e}_1$ and $\mathbf{a}_0$, and as such, the mean angle for this distribution, which is usually denoted by μ, is identically zero—a direct consequence of selecting the intrinsic coordinate system that we did.

In the spirit of [Lanir, 1983], we propose the following definition for our forth invariant for 2D splay:

$$I_{\langle IV\rangle} = \int_{-\pi/2}^{\pi/2} \frac{\exp(-\theta^2/2\varsigma^2)}{\varsigma\sqrt{2\pi}\,\mathrm{erf}(\pi/2\sqrt{2}\varsigma)}\,\mathbf{e}_f(\theta)\cdot\mathbf{Q}^{\mathrm{T}}\mathbf{C}\mathbf{Q}\,\mathbf{e}_f(\theta)\,\mathrm{d}\theta, \tag{13}$$

where ς is akin to α, except that ς is not a standard deviation whose units are radians. A like expression with $\mathbf{C}^2$ replacing $\mathbf{C}$ defines $I_{\langle V\rangle}$. The error function $\mathrm{erf}(x)$ is introduced into these formulæ for reasons that will be made clear shortly. These invariants satisfy the required limits: $\lim_{\varsigma\to 0} I_{\langle IV\rangle}(\varsigma) = I_{IV}$ and $\lim_{\varsigma\to 0} I_{\langle V\rangle}(\varsigma) = I_V$. In Eq. (13), the right-deformation tensor $\mathbf{C}$ is rotated into the local coordinate frame $(1, 2, 3)$ by the mapping $\mathbf{Q}^{\mathrm{T}}\mathbf{C}\mathbf{Q}$, or equivalently, the fiber tangent vector $\mathbf{e}_f$ is rotated into the global coordinate frame (X, Y, Z) by the mapping $\mathbf{Q}\,\mathbf{e}_f$, in accordance with Eq. (11).

3.2 Three-Dimensional Splay Invariants

For transversely isotropic 3D tissues, $\mathbf{e}_f$ is located via spherical coordinates

$$\mathbf{e}_f(\theta,\phi) = \cos(\theta)\,\mathbf{e}_1 + \sin(\theta)(\cos(\phi)\,\mathbf{e}_2 + \sin(\phi)\,\mathbf{e}_3), \tag{14}$$

based on the geometry presented in Fig. 1. Here angles θ and ϕ orient $\mathbf{e}_f$ with respect to the mean-fiber direction $\mathbf{e}_1$ of the embedded frame.

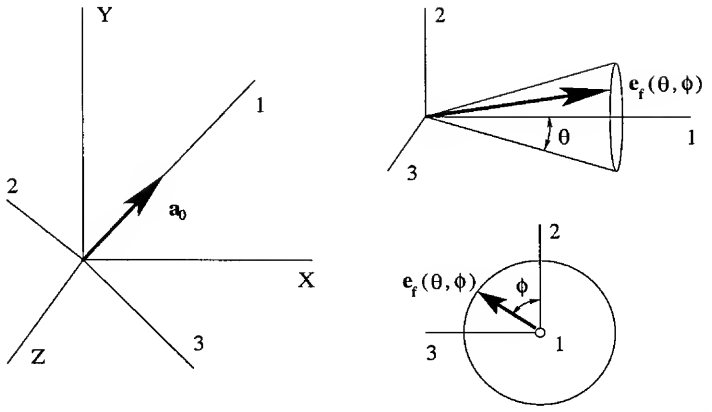

Figure 1 The diagram on the left relates the global coordinates (X, Y, Z) to the local coordinates $(1, 2, 3)$, selected so that the mean-fiber direction $\mathbf{a}_0$ in the Lagrangian frame aligns with the 1 axis. The diagrams on the right illustrate how the unit vector $\mathbf{e}_f$ for a specific fiber within a fiber distribution of a 3D tissue is oriented with respect to the mean-fiber direction $\mathbf{a}_0$ via angles θ and ϕ.

For 3D splay with transverse isotropy, our forth invariant is defined by

$$I_{\langle IV\rangle} = \int_0^{2\pi}\int_{-\pi/2}^{\pi/2} \frac{\exp(-\theta^2/2\varsigma^2)}{\varsigma(2\pi)^{3/2}\,\mathrm{erf}(\pi/2\sqrt{2}\varsigma)}\,\mathbf{e}_f(\theta,\phi)\cdot\mathbf{Q}^{\mathrm{T}}\mathbf{C}\mathbf{Q}\,\mathbf{e}_f(\theta,\phi)\,\mathrm{d}\theta\,\mathrm{d}\phi. \qquad (15)$$

A like formula with $\mathbf{C}^2$ replacing $\mathbf{C}$ defines $I_{\langle V\rangle}$. The Gaussian distribution is independent of ϕ in these invariants, because of an assumption of isotropy in the transverse plane. Once again, $\lim_{\varsigma\to 0} I_{\langle IV\rangle}(\varsigma) = I_{IV}$ and $\lim_{\varsigma\to 0} I_{\langle V\rangle}(\varsigma) = I_V$.

The fact that a right circular cone is used to describe the angular dispersion of individual fibers implies a radial symmetry in the transverse plane, which is consistent with the notion of transverse isotropy. An elliptic cone could be employed if radial symmetry were deemed inappropriate. We will discuss this case later, but we do not derive it.

3.3 Intrinsic Anisotropic Stiffness

We postulate the existence of a material-constant tensor field that we denote as $\boldsymbol{\kappa}$, which serves as a relative (i.e., normalized) stiffness matrix associated with the anisotropic facets of material geometry. For 2D splay, this field is given by

$$\boldsymbol{\kappa}(\varsigma) = \int_{-\pi/2}^{\pi/2} \frac{\exp(-\theta^2/2\varsigma^2)}{\varsigma\sqrt{2\pi}\,\mathrm{erf}(\pi/2\sqrt{2}\varsigma)}\,\mathbf{e}_f(\theta)\otimes\mathbf{e}_f(\theta)\,\mathrm{d}\theta, \qquad (16)$$

and for 3D splay with transverse isotropy, it is given by

$$\boldsymbol{\kappa}(\varsigma) = \int_0^{2\pi}\int_{-\pi/2}^{\pi/2} \frac{\exp(-\theta^2/2\varsigma^2)}{\varsigma(2\pi)^{3/2}\,\mathrm{erf}(\pi/2\sqrt{2}\varsigma)}\,\mathbf{e}_f(\theta,\phi)\otimes\mathbf{e}_f(\theta,\phi)\,\mathrm{d}\theta\,\mathrm{d}\phi, \tag{17}$$

where the global stiffness K introduced in Eq. (6) relates to this intrinsic stiffness $\boldsymbol{\kappa}$ via

$$\mathsf{K} = \mathsf{Q}\,\boldsymbol{\kappa}\,\mathsf{Q}^{\mathrm{T}}. \tag{18}$$

Both of these $\boldsymbol{\kappa}$ matrices obey the required property: $\lim_{\varsigma\to 0}\mathsf{Q}\,\boldsymbol{\kappa}(\varsigma)\mathsf{Q}^{\mathrm{T}} = \mathbf{a}_0\otimes\mathbf{a}_0$, and both of the $\boldsymbol{\kappa}$ matrices are symmetric; therefore, their affiliated K matrices are symmetric, too. Analytic solutions to Eqs. (16 & 17) are provided in Apps. A & B, respectively. The ability to analytically solve for the anisotropic stiffness K means that this theory will be efficient when implemented into finite-element codes. In contrast, the models of[Hurschler et al., 1997], [Sacks, 2000], and [Einstein, 2002] all require a numeric integration of splay, which is more costly to implement.

The coefficient $1/\mathrm{erf}(\pi/2\sqrt{2}\varsigma)$ is introduced into Eqs. (16 & 17) to force the trace of $\boldsymbol{\kappa}$ (and therefore of K) to equal the trace of $\mathbf{a}_0\otimes\mathbf{a}_0$ (viz., $\mathrm{tr}(\mathbf{a}_0\otimes\mathbf{a}_0) = 1$), which is the only non-zero invariant of tensor $\mathbf{a}_0\otimes\mathbf{a}_0$. Alternatively, this coefficient can be viewed as that scaling factor which is required to change the limits of integration from $\int_{-\infty}^{\infty}$ to $\int_{-\pi/2}^{\pi/2}$ in the Gaussian distributions present in these formulæ.

3.3.1 An Approximation The non-zero components of the analytic solutions to the intrinsic stiffness matrices listed in the appendices are expressed in terms of error functions with complex arguments (e.g., $\mathrm{erf}(z)$, $z\in\mathbb{C}$). Because this function is not found in most, standard, computer, math libraries, we introduce a simple approximation to the analytic results derived in these appendices that one can readily employ; it being,

$$\boldsymbol{\kappa}(\varsigma) \approx \begin{bmatrix} \frac{1}{2}(1+\mathrm{e}^{-2\varsigma^2}) & 0 & 0 \\ 0 & \frac{f}{2}(1-\mathrm{e}^{-2\varsigma^2}) & 0 \\ 0 & 0 & \frac{1-f}{2}(1-\mathrm{e}^{-2\varsigma^2}) \end{bmatrix}, \quad 0\le f\le 1, \tag{19}$$

which is in keeping with the constraint that $\mathrm{tr}\,\boldsymbol{\kappa} = 1$. Parameters $f = 0$ and $f = 1$ apply to 2D splay with the normal to the membrane being in the 2- and 3-directions, respectively, while $f = \frac{1}{2}$ applies for 3D splay with transverse isotropy. Splay will be orthotropic whenever $f \neq \frac{1}{2}$; specifically, there will be an elliptic symmetry in the transverse plane.

The analytic (App. A) and approximate (Eq. 19) solutions for $\boldsymbol{\kappa}$ are contrasted in Fig. 2 for 2D splay, while the formulæ in App. B and Eq. (19) are contrasted in Fig. 3 for 3D splay with transverse isotropy. As a result, one can easily justify using the approximate solution stated in Eq. (19) over its analytic counterparts derived in the appendices, especially since selecting a Gaussian distribution to describe fiber dispersion was an assumption in the first place.

Substituting Eq. (19) into Eq. (18) quantifies the global stiffness matrix K that appears in the elastic model of Eqs. (9 & 10) and its associated invariants in Eq. (6).

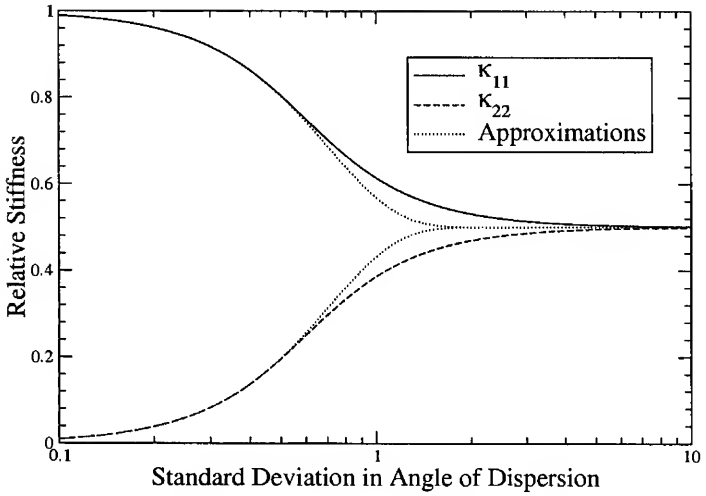

Figure 2 Plots of relative stiffness vs. standard deviation in the angle of fiber dispersion for 2D splay, as determined by Eq. (19) with $f = 1$ for the approximate solutions, and by Eqs. (A4 & A5) for the analytic solutions.

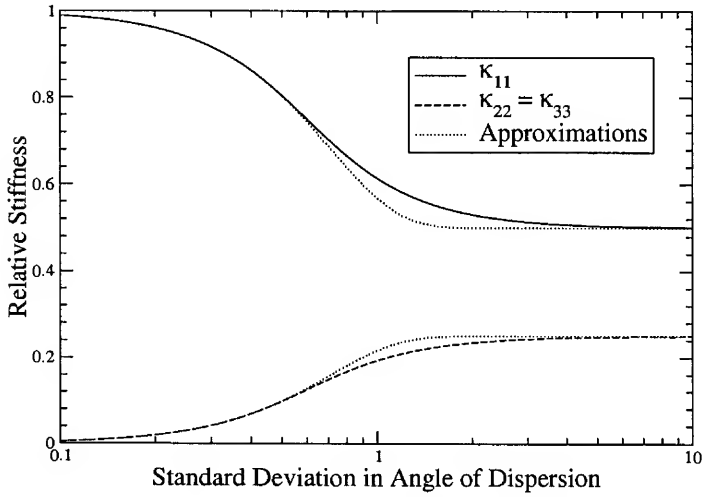

Figure 3 Plots of relative stiffness vs. standard deviation in the angle of fiber dispersion for transversely isotropic 3D splay, as determined by Eq. (19) with $f = ½$ for the approximate solutions, and by Eqs. (B4 & B5) for the analytic solutions.

4 Elasticity for Finite Elements

Soft tissues are generally considered to be incompressible or nearly incompressible. In a finite element analysis that involves incompressibility, a standard displacement based interpolation method leads to ill-conditioning of the numerics [Malkus and Hughes, 1978]. Anticipating like difficulties, following [Flory, 1961], we seek to decouple pressure from displacement. This decoupling is compatible with two-field displacement-pressure interpolations that avoid volumetric locking in particular, and numerical ill-conditioning in general.

Adopting the approach and notation of [Simo and Hughes, 1998, pp. 358–364], we define

$$J = \det \mathsf{F} = \tfrac{\varrho_0}{\varrho}, \quad \bar{\mathsf{F}} = J^{-1/3}\mathsf{F}, \quad \bar{\mathsf{C}} = \bar{\mathsf{F}}^{\mathrm{T}}\bar{\mathsf{F}}, \quad \bar{\mathsf{B}} = \bar{\mathsf{F}}\bar{\mathsf{F}}^{\mathrm{T}}, \tag{20}$$

so that $\det \bar{\mathsf{F}} = 1$, and therefore, $\det \bar{\mathsf{B}} = \det \bar{\mathsf{C}} = 1$. Consequently, the strain-energy density W is assumed to decouple as follows:

$$\varrho_0 W(\mathsf{C}) = \overline{W}(J) + \widetilde{W}(\bar{\mathsf{C}}) + \widehat{W}(\mathsf{K}, \bar{\mathsf{C}}), \tag{21}$$

where $\overline{W}$, $\widetilde{W}$, and $\widehat{W}$ are the dilational, distortional-isotropic, and distortional-anisotropic strain energies, respectively.

The above definitions allow the general constitutive equation for elasticity stated in Eq. (8) to be recast as

$$\mathsf{S} = J\frac{\partial \overline{W}(\Theta)}{\partial \Theta}\mathsf{C}^{-1} + 2J^{-2/3}\left(\mathrm{DEV}\left[\frac{\partial \widetilde{W}(\bar{\mathsf{C}})}{\partial \bar{\mathsf{C}}}\right] + \mathrm{DEV}\left[\frac{\partial \widehat{W}(\mathsf{K}, \bar{\mathsf{C}})}{\partial \bar{\mathsf{C}}}\right]\right), \tag{22}$$

so that, when pulled forward into the Eulerian frame, it becomes

$$\tau = J\frac{\partial \overline{W}(\Theta)}{\partial \Theta}\mathsf{I} + 2\left(\mathrm{dev}\left[\bar{\mathsf{F}}\frac{\partial \widetilde{W}(\bar{\mathsf{C}})}{\partial \bar{\mathsf{C}}}\bar{\mathsf{F}}^{\mathrm{T}}\right] + \mathrm{dev}\left[\bar{\mathsf{F}}\frac{\partial \widehat{W}(\mathsf{K}, \bar{\mathsf{C}})}{\partial \bar{\mathsf{C}}}\bar{\mathsf{F}}^{\mathrm{T}}\right]\right), \tag{23}$$

wherein

$$\mathrm{DEV}[\bullet] = (\bullet) - \tfrac{1}{3}\,\mathrm{tr}((\bullet)\mathsf{C})\mathsf{C}^{-1} \quad \text{and} \quad \mathrm{dev}[\bullet] = (\bullet) - \tfrac{1}{3}\,\mathrm{tr}(\bullet)\mathsf{I} \tag{24}$$

are the respective Lagrangian and Eulerian deviatoric operators. Tensors $\bar{\mathsf{F}}$ and $\Theta\mathsf{I}$ are the deviatoric (volume preserving) and dilational (volume changing) parts of the deformation gradient F, respectively. Although $\Theta \equiv J$ in a mathematical sense, we follow the admonition of Simo and Hughes and maintain their distinction, to remind ourselves that displacement and pressure are to be interpolated separately in finite-element codes suitable for soft-tissue analysis.

4.1 A Simple Model

The spherical strain-energy model advocated by [Simo and Hughes, 1998, pg. 361], and adopted, for example, by [Kaliske, 2000], is

$$\overline{W}(\Theta) = \kappa\tfrac{1}{2}(\tfrac{1}{2}(\Theta^2 - 1) - \ln\Theta), \tag{25}$$

where κ is the bulk modulus. Equation (25) is recommended because it is a convex function[4], and because its gradient leads to a second-order accurate approxima-

[4] $\partial^2 \overline{W}/\partial\Theta^2 = \frac{1}{2}\kappa(1 + \Theta^{-2}) > 0$, as $\Theta > 0$ due to the conservation of mass

tion of the [Hencky, 1928] definition for dilatation[5] [Freed, 2004]. Equation (25) is appropriate for mean-dilation (or reduced/selective) integration schemes used in some finite-element codes.

Equation (25) does not, however, fit the constraint criteria of the u/p finite-element scheme advocated by [Sussman and Bathe, 1987]. Thus, if this interpolation scheme is adopted, then

$$\overline{\mathcal{W}}(\Theta) = \kappa\tfrac{1}{2}(J-1)^2, \tag{26}$$

must be employed as the dilational strain-energy model. In these codes there is no distinction made between J and Θ.

Seeking an isotropic contribution to the deviatoric strain energy with attributes akin to those affiliated with the dilational part (viz., a convex function whose gradient produces a second-order accurate approximation of true strain), we assign

$$2\widetilde{\mathcal{W}}(\bar{\mathsf{C}}) = \mu\tfrac{1}{4}(\operatorname{tr}\bar{\mathsf{C}} + \operatorname{tr}\bar{\mathsf{C}}^{-1} - 6), \tag{27}$$

where μ is the shear modulus, with $\bar{\mathsf{C}}^{-1} = \{\bar{\mathsf{C}}^2 - \operatorname{tr}(\bar{\mathsf{C}})\bar{\mathsf{C}} + \frac{1}{2}[(\operatorname{tr}\bar{\mathsf{C}})^2 - \operatorname{tr}\bar{\mathsf{C}}^2]\mathsf{I}\}/\det\bar{\mathsf{C}}$ from the Cayley-Hamilton theorem. Tensor $\bar{\mathsf{C}}^{-1}$ exists because $\det\bar{\mathsf{C}} = 1$; consequently, $I_{II}(\bar{\mathsf{C}}) = \frac{1}{2}[(\operatorname{tr}\bar{\mathsf{C}})^2 - \operatorname{tr}\bar{\mathsf{C}}^2] = \operatorname{tr}\bar{\mathsf{C}}^{-1} = I_I(\bar{\mathsf{C}}^{-1})$. A [Mooney, 1940] material has different material constants assigned to invariants $\operatorname{tr}\bar{\mathsf{C}}$ and $\operatorname{tr}\bar{\mathsf{C}}^{-1}$, in general, and in this sense, our model is a Mooney material of special form.

For an anisotropic contribution to the deviatoric strain energy, going back to the precept that energy is the area under a force/displacement curve, we advocate that

$$\widehat{\mathcal{W}}(\mathsf{K}, \bar{\mathsf{C}}) = \int_1^{[\operatorname{tr}(\mathsf{K}\bar{\mathsf{C}})]^{1/2}} \sigma(\lambda)\,\mathrm{d}\lambda, \tag{28}$$

where the fiber stress σ is allowed to be an arbitrary function of fiber stretch λ; it is generally nonlinear in biological tissues. The upper limit of integration is the forth invariant, as it pertains to the deviatoric part of the deformed state. In order for this strain-energy function to be convex, it is necessary that $E_t(\lambda) > \sigma_t(\lambda)$ for all $\lambda > 0$, wherein

$$E_t(\lambda) = \frac{\mathrm{d}\sigma(\lambda)}{\mathrm{d}\lambda} \quad \text{and} \quad \sigma_t(\lambda) = \frac{\sigma(\lambda)}{\lambda}, \tag{29}$$

which are the fiber tangent-modulus and true-stress, respectively, with the fiber stretch λ being quantified by

$$\lambda = (\operatorname{tr}(\mathsf{K}\bar{\mathsf{C}}))^{1/2} = (\operatorname{tr}(\bar{\mathsf{F}}\mathsf{K}\bar{\mathsf{F}}^{\mathrm{T}}))^{1/2}. \tag{30}$$

A physiologically based material model for $\sigma(\lambda)$ has recently been derived by [Freed and Doehring, 2004] that applies to crimped collagen fibers, which we have extended to meet our needs in App. C.

[5] $e = \ln\det\mathsf{F} \approx \frac{1}{2}(\det\mathsf{F} - \det\mathsf{F}^{-1})$

Substituting the strain energies of Eqs. (25–28) into Eq. (22) produces an elastic constitutive model suitable for soft-tissue mechanics that when expressed in the Lagrangian frame becomes

$$\mathsf{S} = \kappa J\,\tfrac{1}{2}(\Theta - \Theta^{-1})\,\mathsf{C}^{-1} + \mu J^{-2/3}\,\mathrm{DEV}[\tfrac{1}{4}(\mathsf{I} - \bar{\mathsf{C}}^{-2})] + \sigma_t(\lambda) J^{-2/3}\,\mathrm{DEV}[\mathsf{K}], \quad (31)$$

or equivalently, when substituted into Eq. (23), becomes

$$\tau = \kappa J\,\tfrac{1}{2}(\Theta - \Theta^{-1})\,\mathsf{I} + \mu\,\mathrm{dev}[\tfrac{1}{4}(\bar{\mathsf{B}} - \bar{\mathsf{B}}^{-1})] + \sigma_t(\lambda)\,\mathrm{dev}[\bar{\mathsf{F}}\mathsf{K}\bar{\mathsf{F}}^{\mathrm{T}}], \quad (32)$$

when expressed in the Eulerian frame. The strain measure $\frac{1}{2}(\Theta - \Theta^{-1})$ is a second-order accurate approximation of Hencky's dilational strain field $\ln \det \mathsf{F}$, while the strain tensor $\frac{1}{4}(\mathsf{B} - \mathsf{B}^{-1})$ is a second-order accurate approximation of the true-strain field $\ln \mathsf{V}$ [Freed, 2004]. Each contribution is convex provided that $\kappa > 0$, $\mu > 0$, and $E_t(\lambda) > \sigma_t(\lambda)$ for all λ.

4.2 Tangent Moduli

The relationship between S and C in Eq. (31) is nonlinear. To obtain a finite-element solution with an iterative Newton-type solution process, that relationship must be linearized with respect to an incremental displacement. This involves the specification of a tangent modulus M.[6] To obtain this tangent, stress S is linearized over some time interval $[t_n, t_{n+1}]$ such that $\mathsf{S}_{n+1} = \mathsf{S}_n + \mathsf{M}_n \Delta\mathsf{E}$ with $\Delta\mathsf{E} = \mathsf{E}_{n+1} - \mathsf{E}_n = \frac{1}{2}(\mathsf{C}_{n+1} - \mathsf{C}_n) = \mathsf{F}_n^{\mathrm{T}}\hat{\mathsf{E}}(\mathbf{x}_n; t_n, t_{n+1})\mathsf{F}_n$. Said differently, the tangent modulus corresponds to the slope affiliated with a forward-Euler integration step, and since it depends on step number n, it needs to be re-evaluated at each step along the solution path.

Tensor $\mathsf{M}_n = 2\partial\mathsf{S}/\partial\mathsf{C}_n = 4\varrho_0\partial^2 W/\partial\mathsf{C}_n\partial\mathsf{C}_n$ defines the tangent modulus in the Lagrangian frame, which can be pulled forward, component by component, into an Eulerian frame (commonly called the updated Lagrangian frame) according to the mapping $m^n_{ijk\ell} = F^n_{il}F^n_{jJ}F^n_{kK}F^n_{\ell L}M^n_{IJKL}$ at the n^{th} time step. Constructing the components of M_n in Voigt notation is addressed in App. D.

From Eq. (21), suppressing the subscript n designating step number, the tangent modulus takes on the form

$$\mathsf{M} = \bar{\mathsf{M}}(\Theta) + \tilde{\mathsf{M}}(\bar{\mathsf{C}}) + \hat{\mathsf{M}}(\mathsf{K}, \bar{\mathsf{C}}), \quad (33)$$

where, through an application of the chain rule, one obtains

$$\begin{aligned}
\bar{\mathsf{M}} &= 4\,\frac{\partial^2 \bar{W}(\Theta)}{\partial\mathsf{C}\,\partial\mathsf{C}} = 4\left(\frac{\partial^2 \bar{W}(\Theta)}{\partial\Theta^2}\,\frac{\partial\Theta}{\partial\mathsf{C}} \otimes \frac{\partial\Theta}{\partial\mathsf{C}} + \frac{\partial \bar{W}(\Theta)}{\partial\Theta}\,\frac{\partial^2\Theta}{\partial\mathsf{C}\,\partial\mathsf{C}}\right),\\
\tilde{\mathsf{M}} &= 4\,\frac{\partial^2 \tilde{W}(\bar{\mathsf{C}})}{\partial\mathsf{C}\,\partial\mathsf{C}} = 4\left(\left(\frac{\partial\bar{\mathsf{C}}}{\partial\mathsf{C}}\right)^{\mathrm{T}} : \frac{\partial^2 \tilde{W}(\bar{\mathsf{C}})}{\partial\bar{\mathsf{C}}\,\partial\bar{\mathsf{C}}} : \frac{\partial\bar{\mathsf{C}}}{\partial\mathsf{C}} + \frac{\partial \tilde{W}(\bar{\mathsf{C}})}{\partial\bar{\mathsf{C}}} : \frac{\partial^2\bar{\mathsf{C}}}{\partial\mathsf{C}\,\partial\mathsf{C}}\right),\\
\hat{\mathsf{M}} &= 4\,\frac{\partial^2 \hat{W}(\mathsf{K}, \bar{\mathsf{C}})}{\partial\mathsf{C}\,\partial\mathsf{C}} = 4\left(\left(\frac{\partial\bar{\mathsf{C}}}{\partial\mathsf{C}}\right)^{\mathrm{T}} : \frac{\partial^2 \hat{W}(\mathsf{K}, \bar{\mathsf{C}})}{\partial\bar{\mathsf{C}}\,\partial\bar{\mathsf{C}}} : \frac{\partial\bar{\mathsf{C}}}{\partial\mathsf{C}} + \frac{\partial \hat{W}(\mathsf{K}, \bar{\mathsf{C}})}{\partial\bar{\mathsf{C}}} : \frac{\partial^2\bar{\mathsf{C}}}{\partial\mathsf{C}\,\partial\mathsf{C}}\right),
\end{aligned} \quad (34)$$

[6] The tangent modulus M is often denoted as C, which we use to denote the right-deformation tensor of Cauchy.

with

$$\frac{\partial \bar{C}_{ij}}{\partial C_{k\ell}} = J^{-2/3}(I_{ik}I_{j\ell} - \tfrac{1}{3}\, C_{ij}C^{-1}_{k\ell}), \tag{35}$$

and

$$\frac{\partial^2 \bar{C}_{ij}}{\partial C_{k\ell}\,\partial C_{mn}} = \tfrac{1}{3}J^{-2/3}\Big(C_{ij}(C^{-1}_{km}C^{-1}_{\ell n} + \tfrac{1}{3}C^{-1}_{k\ell}C^{-1}_{mn}) - I_{ik}I_{j\ell}C^{-1}_{mn} - C^{-1}_{k\ell}I_{im}I_{jn}\Big). \tag{36}$$

For the preferred volumetric strain energy in Eq. (25), which can be implemented into finite-element codes that use a reduced/selective integration scheme [Malkus and Hughes, 1978], one arrives at the following pressure tangent modulus[7]

$$\bar{\mathsf{M}} = 2\kappa\left((1+\Theta^{-2})\frac{\partial \Theta}{\partial \mathsf{C}} \otimes \frac{\partial \Theta}{\partial \mathsf{C}} + (\Theta - \Theta^{-1})\frac{\partial^2 \Theta}{\partial \mathsf{C}\,\partial \mathsf{C}}\right), \tag{37}$$

where the gradients $\partial\Theta/\partial\mathsf{C} \otimes \partial\Theta/\partial\mathsf{C}$ and $\partial^2\Theta/\partial\mathsf{C}\,\partial\mathsf{C}$ are handled by the element technology of the particular finite element being employed. Alternatively, in an u/p formulation [Sussman and Bathe, 1987], the pressure tangent modulus corresponding to Eq. (26) is given by[8]

$$\bar{\mathsf{M}} = \kappa J\Big(J\,\mathsf{C}^{-1}\otimes\mathsf{C}^{-1} + (1-J)(2\mathsf{C}^{-1}\boxtimes\mathsf{C}^{-1} - \mathsf{C}^{-1}\otimes\mathsf{C}^{-1})\Big), \tag{38}$$

where now the gradients $\partial\Theta/\partial\mathsf{C} \otimes \partial\Theta/\partial\mathsf{C}$ and $\partial^2\Theta/\partial\mathsf{C}\,\partial\mathsf{C}$ are handled by us, the constitutive developers, as there is no distinction made between Θ and J in these codes.

The isotropic tangent modulus corresponding to Eq. (27) is determined to be

$$\begin{aligned}\tilde{\mathsf{M}} = \mu\Big\{J^{2/3}\Big[&\mathsf{C}^{-1}\boxtimes\mathsf{C}^{-2} - \tfrac{1}{3}(\mathsf{C}^{-1}\otimes\mathsf{C}^{-2} + \mathsf{C}^{-2}\otimes\mathsf{C}^{-1}) + \tfrac{1}{9}(\operatorname{tr}\mathsf{C}^{-1})\,\mathsf{C}^{-1}\otimes\mathsf{C}^{-1}\Big] \\ &+ \tfrac{1}{6}\Big[(J^{-2/3}\operatorname{tr}\mathsf{C} - J^{2/3}\operatorname{tr}\mathsf{C}^{-1})(\mathsf{C}^{-1}\boxtimes\mathsf{C}^{-1} + \tfrac{1}{3}\mathsf{C}^{-1}\otimes\mathsf{C}^{-1}) \\ &\quad - \mathsf{C}^{-1}\otimes(J^{-2/3}\mathsf{I} - J^{2/3}\mathsf{C}^{-2}) - (J^{-2/3}\mathsf{I} - J^{2/3}\mathsf{C}^{-2})\otimes\mathsf{C}^{-1}\Big]\Big\}.\end{aligned} \tag{39}$$

Lastly, the anisotropic tangent modulus corresponding to Eq. (28) is found to be given by

$$\begin{aligned}\hat{\mathsf{M}} = J^{-2/3}\Big\{&(E_t(\lambda) - \sigma_t(\lambda))\Big(J^{-2/3}\lambda^{-2}\,\mathsf{K}\otimes\mathsf{K} \\ &\quad - \tfrac{1}{3}(\mathsf{K}\otimes\mathsf{C}^{-1} + \mathsf{C}^{-1}\otimes\mathsf{K}) + \tfrac{1}{9}J^{2/3}\lambda^2\,\mathsf{C}^{-1}\otimes\mathsf{C}^{-1}\Big) \\ &+ \tfrac{2}{3}\sigma_t(\lambda)\Big(J^{2/3}\lambda^2(\mathsf{C}^{-1}\boxtimes\mathsf{C}^{-1} + \tfrac{1}{3}\mathsf{C}^{-1}\otimes\mathsf{C}^{-1}) - \mathsf{K}\otimes\mathsf{C}^{-1} - \mathsf{C}^{-1}\otimes\mathsf{K}\Big)\Big\}.\end{aligned} \tag{40}$$

[7] These tensor gradients are useful when deriving the subsequent tangent moduli:

$$\frac{\partial \mathsf{Z}}{\partial \mathsf{Z}} = \mathsf{I}\boxtimes\mathsf{I} \quad \& \quad \frac{\partial \mathsf{Z}^{-1}}{\partial \mathsf{Z}} = -\mathsf{Z}^{-1}\boxtimes\mathsf{Z}^{-1} \quad \text{given that} \quad \mathsf{Z} = \mathsf{Z}^{\mathrm{T}}.$$

[8] The outer-dyadic tensor product $[\![\mathsf{A}\otimes\mathsf{B}]\!]_{ijk\ell} = A_{ij}B_{k\ell}$, and the inner-dyadic tensor product $[\![\mathsf{A}\boxtimes\mathsf{B}]\!]_{ijk\ell} = \tfrac{1}{4}(A_{ik}B_{j\ell} + A_{i\ell}B_{jk} + A_{jk}B_{i\ell} + A_{j\ell}B_{ik})$, are established in App. D.

5 Collagen Models

The fiber tangent modulus $E_t(\lambda)$ and true stress $\sigma_t(\lambda)$ present in Eq. (40) are defined in Eq. (29), whose stretch λ is established in Eq. (30). It is worth noting that the terms in the fourth-rank tensor representing the anisotropic tangent modulus are completely independent of the specific collagen fiber model chosen. This implies that a modification of fiber stress-strain law requires no re-formulation of the constitutive tangent matrix, making the model very flexible for different types of soft tissues. This is not the case with constitutive models represented by Eq. (1).

In the Examples section that follows, two collagen stress-strain models are used. The first is the rule adopted by [Billiar and Sacks, 2000b] for aortic valve tissue; it being,

$$\sigma(\lambda) = A(\mathrm{e}^{B(\lambda^2-1)/2} - 1), \tag{41}$$

thus the two required terms in Eq. (40) are

$$\sigma_t(\lambda) = A\lambda^{-1}(\mathrm{e}^{B(\lambda^2-1)/2} - 1) \quad \text{and} \quad E_t(\lambda) = AB\lambda\mathrm{e}^{B(\lambda^2-1)/2}. \tag{42}$$

As an alternative to this phenomenological model, we also employ the structural model of [Freed and Doehring, 2004] that is based on the physiology of crimped collagen fibers. An adaptation of their algorithm is given in App. C (see Alg. 1). Specifically, given a fiber stretch λ, this model returns the true stress σ/λ and tangent modulus $\mathrm{d}\sigma/\mathrm{d}\lambda$ of the fiber. There are four physiologic parameters (material constants defined at the top of the algorithm) that the user must supply.

To implement either of these two models in finite elements, or any other model for that matter, it is sufficient to change the lines of code corresponding to the scalar values $E_t(\lambda)$ and $\sigma_t(\lambda)$. This opens up the possibility of coding the material model once and selecting an appropriate fiber model with a passed parameter.

6 Examples

We offer our invariant theory as a computationally efficient alternative to statistical structural models of the type represented by Eq. (1).

In the examples that follow, we match Eq. (31) to biaxial data for fresh aortic valve tissue. These data were generously supplied by Dr. Sacks from the Engineered Tissue Mechanics Laboratory at the University of Pittsburgh, and have been reported on elsewhere [Billiar and Sacks, 2000a]. In the first example, we adopt an exponential fiber stress-strain rule—the same phenomenological model used by [Billiar and Sacks, 2000b]. In the second example, we adopt a structurally based collagen fiber model recently derived by [Freed and Doehring, 2004].

The original data were provided in the format of Lagrangian membrane tension; that is, force per unit reference length. To characterize the constitutive model, it was necessary to convert the data to Lagrangian stress. Thus, a thickness of 0.6 mm was assumed. It must also be noted that these data do not comprise a complete biaxial set, in the sense that there were finite off-axis deformation terms (i.e., $F_{12} \neq F_{21} \neq 0$, cf. Fig. 4) with no concomitant measurement of an off-axis stress.

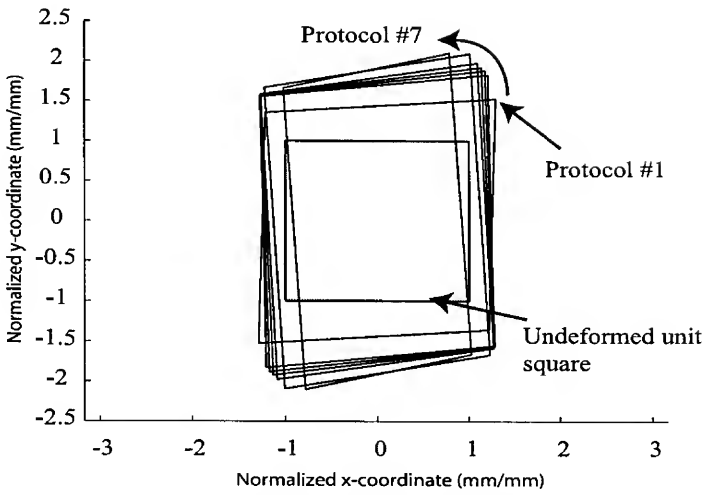

Figure 4 Mapping of a unit square to the current configuration, corresponding to the last data point of each of the seven protocols of [Billiar and Sacks, 2000a]. Note that there exist finite $F_{12} \neq F_{21}$ terms.

As such, is was necessary to convert Eq. (31) into its first Piola-Kirchhoff stress (i.e. $\mathbf{P} = \mathbf{FS}$) counterpart for parameter estimation.

An adaptive grid refinement (AGR) global optimization algorithm was implemented in Mathematica™ (Wolfram Research Incorporated, Champagne, IL), using a commercially available global optimization algorithm (Global Optimization, Loehle Enterprises, Naperville, IL) [Doehring et al., 2004]. Parameters were simultaneously fit to five separate biaxial load protocols, corresponding to fiber–to–cross-fiber membrane stress ratios of 30:60, 45:60, 60:60, 60:45, and 60:30 N/m. These were the same protocols used to fit the data in the original publications by [Billiar and Sacks, 2000a, Billiar and Sacks, 2000b]. During the estimation process, the membranes were considered to be incompressible and the shear modulus pertaining to the isotropic response was set to zero. The objective function for the global minimum was defined as

$$\text{error} = \sum_{j=1}^{5} \left(\frac{\sum_{i=1}^{N_j} \left(P_{11}^{model} - P_{11}^{data} \right)_{ij}^2}{\sum_{i=1}^{N_j} \left(P_{11}^{data} \right)_{ij}^2} + \frac{\sum_{i=1}^{N_j} \left(P_{22}^{model} - P_{22}^{data} \right)_{ij}^2}{\sum_{i=1}^{N_j} \left(P_{22}^{data} \right)_{ij}^2} \right), \tag{43}$$

where P_{11} corresponds to the fiber direction, P_{22} corresponds to the cross-fiber direction, and N_j represents the number of data points for the j^{th} protocol.

6.1 Exponential Fiber Model

In this example, we specifically compare our constitutive model to both the data and to a statistical structural model with an exponential fiber stress that was proposed in [Billiar and Sacks, 2000b] and implemented by [Einstein, 2002] as

$$\mathbf{S} = J^{-2/3}\mathrm{DEV}\left[\int_{-\pi/2}^{\pi/2} S_f(\theta)\, R(\theta)\, \mathbf{N}(\theta)\otimes\mathbf{N}(\theta)\, d\theta\right] \tag{44}$$

where the fiber stress-strain law $S_f(\theta)$ and the probability density function $R(\theta)$ are given by

$$S_f(\theta) = A\left(e^{B\left(\mathbf{N}(\theta)\cdot\bar{\mathbf{C}}\mathbf{N}(\theta)-1\right)/2} - 1\right) \quad \text{and} \quad R(\theta) = \frac{\exp(-\theta^2/2\alpha^2)}{\alpha\sqrt{2\pi}}. \tag{45}$$

The fiber tangent modulus $E_t(\lambda)$ and true stress $\sigma_t(\lambda)$ for Eq. (31) are given by (42).

Optimized parameters for the constitutive model based on our new invariant theory (Eqs. 31 & 42) were: $A = 0.007$, $B = 21.6$, and $\varsigma = 0.795$. Parameters for the constitutive model based on the statistical structure of Eqs. (44 & 45) were: $A = 0.045$, $B = 21.0$, and $\alpha = 0.192$. Note that although the units for α in Eq. (45) are radians, our ς parameter in Eq. (19) is not strictly an angle. To force the consistency constraint $\lim_{\varsigma\to 0}\mathbf{Q}\,\boldsymbol{\kappa}(\varsigma)\mathbf{Q}^{\mathrm{T}} = \mathbf{a}_0\otimes\mathbf{a}_0$ required us to introduce a scaling factor of $1/\mathrm{erf}(\pi/2\sqrt{2}\varsigma)$ into $R(\theta)$.

Overall, the fit was quite good for both models (see Fig. 5). The error calculated via Eq. (43) for the invariant model of Eqs. (31 & 42) was 0.40, as opposed to an error of 0.45 for the model of Eqs. (44 & 45). On average, Eqs. (31 & 42) tended to fit the fiber-direction stress slightly better, while Eqs. (44 & 45) tended to fit the cross-fiber stress slightly better. With regard to our constitutive model only, the toe-region of the stress-strain curve (commonly viewed as a transition between the extinction of collagen crimp and the linear behavior of straightened collagen) was slightly under-predicted in the fiber direction and over-predicted in the cross-fiber direction.

6.2 Crimped Collagen Model

Because the modulus $E_t(\lambda)$ and true stress $\sigma_t(\lambda)$ are generic scalar components of the anisotropic tangent modulus in Eq. (40), we are free to adopt any reasonable fiber stress-strain rule, without making the complexity due to tangent modulus construction prohibitive. This is a desirable precondition for finite-element analysis.

As our second example, consider the micro-structurally based collagen fiber stress-strain rule based on the physiology of crimped collagen fibers that was recently proposed by[Freed and Doehring, 2004] (Alg. 1 in App. C). This is an algorithm for the elastic response of crimped collagen fibers, based on the observation that fibril crimp has a three-dimensional structure at the μm scale whose geometry can be approximated as a cylindrical helix. For pre-failure analysis, the model is

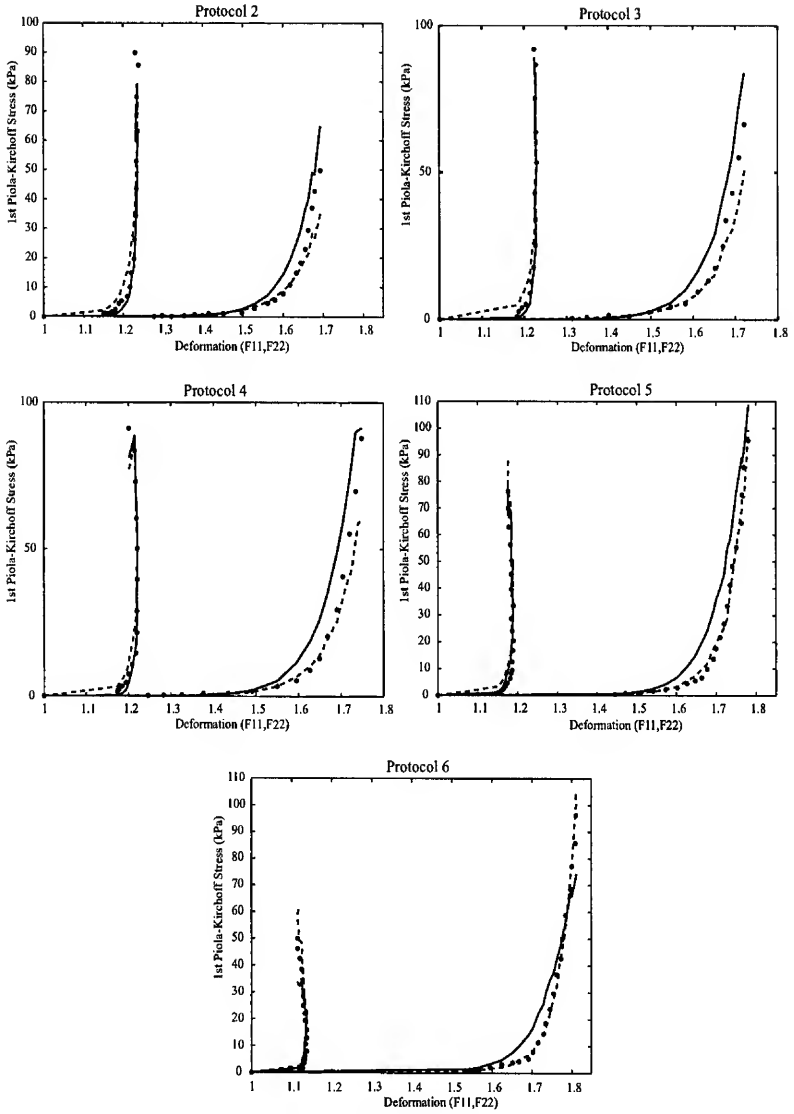

Figure 5 Constitutive model fit to biaxial data from fresh aortic valve tissue: exponential fiber stress-strain rule (left: fiber direction, right: cross-fiber direction). Dots are the original data. Solid lines are from our constitutive model Eqs. (31 & 42). Dashed lines are from the statistical model in Eq. (44) with Eq. (45) for the stress/stretch law.

defined in terms of three physiologic parameters: the initial normalized wavelength of the crimp H_0/r_0, the initial normalized amplitude of the crimp R_0/r_0, and the elastic modulus of the collagen fiber in the linear region E_f. Parameters H_0 and R_0 are normalized with respect to fibril radius r_0.

Values for these parameters were estimated at: $H_0/r_0 = 14.4$, $R_0/r_0 = 2.19$, $E_f = 10.6$MPa, and $\varsigma = 0.768$. Overall, the fit of this variation of our constitutive model was excellent (see Fig. 6), with an error of 0.37. Only the predictions for the sixth protocol have a significant difference from the data.

7 Finite Element Implementation

Equation (31) and Alg. 1 from App. C was implemented into Adina™ (Adina R&D Inc., Watertown, MA). A 10×10 mm square of tissue was meshed with 1764 nodes and 1200 linear solid elements with constant pressure interpolation. A two-field pressure/displacement interpolation was utilized [Sussman and Bathe, 1987]. Displacement boundary conditions were applied to edge nodes. To characterize the full range of behavior, the load was divided into 100 load steps. Simulations were performed for three biaxial stretch ratios: $\lambda_{11}:\lambda_{22} = 1.2{:}1.4$, $1.1{:}1.4$, and $1.0{:}1.4$. The solutions were obtained using a full-Newton method with a sparse equation solver. CPU times were 154, 149, and 150 seconds run on a Linux box containing a single 2.4 GHz Pentium IV processor. In addition to the parametric values stated earlier, the following isotropic moduli were assigned: $\kappa = 20$MPa and $\mu = 500$Pa. There was excellent agreement between the FEA and theoretical solutions (see Fig. 7), with essentially no detectable error.

8 Conclusion

We have proposed an efficient, invariant-based alternative to structural constitutive equations that accounts for a statistical dispersion of fibers. In contrast to existing models, our new invariant theory easily handles a 3D fiber population with a single mean preferred direction. The invariant theory is based on a novel closed-form 'splay invariant' that requires a single parameter in the 2D case, and two parameters in the 3D case. The model is polyconvex, and fits biaxial data for aortic-valve tissue better than existing aortic-valve models. A modification in the fiber stress-strain law requires no re-formulation of the constitutive tangent matrix, making the model flexible for different types of soft tissues. Most importantly, the model is computationally expedient in a finite-element analysis.

Acknowledgements The authors take this opportunity to thank Prof. Michael Sacks at the University of Pittsburgh for providing us with his experimental data, and to Dr. Todd Doehring and Mr. Dimitri Deserranno at the Cleveland Clinic for many delightful discussions on this and related topics.

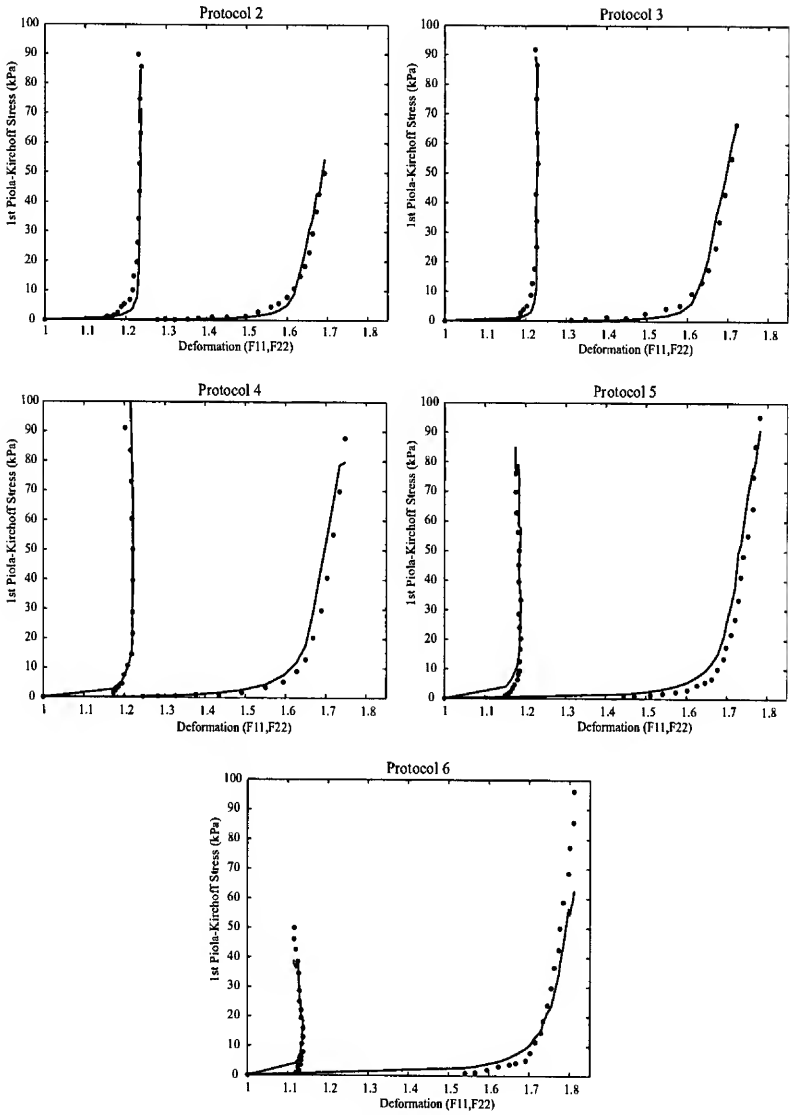

Figure 6 Constitutive model fit to biaxial data from fresh aortic-valve tissue: fiber crimp stress-strain rule (left: fiber direction, right: cross-fiber direction). Dots are the original data. Solid lines are our constitutive model Eq. (31) using Alg. 1 from App. C for the stress/stretch law.

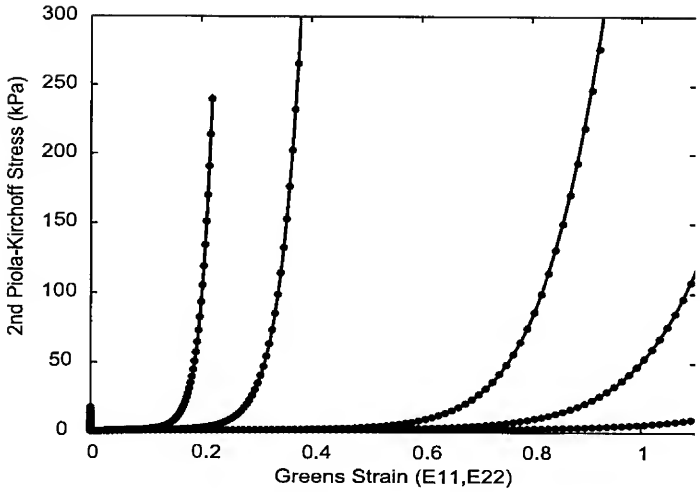

Figure 7 Finite-element simulation of three biaxial stretch ratios: $\lambda_{11}:\lambda_{22}$ = 1.2:1.4, 1.1:1.4, and 1.0:1.4 (solid lines). Left: fiber direction, right: cross-fiber direction). Dots are theoretical solutions.

Appendices

The primary reason for adopting a Gaussian distribution to describe fiber splay is that the corresponding stiffness matrix $\boldsymbol{\kappa}$ can be computed analytically. Alternatively, [Hurschler et al., 1997] have employed a von Mises distribution for splay in conjunction with a Weibull distribution for crimp that they collectively solve numerically.

A Two-Dimensional Splay

We recall that our local coordinate system was chosen so that

$$\mathbf{a}_0 = \begin{Bmatrix} 1 \\ 0 \\ 0 \end{Bmatrix}, \quad \mathbf{e}_f = \begin{Bmatrix} \cos\theta \\ \sin\theta \\ 0 \end{Bmatrix}, \tag{A1}$$

and as such

$$\mathbf{e}_f \otimes \mathbf{e}_f = \begin{bmatrix} \cos^2\theta & \sin\theta\cos\theta & 0 \\ \sin\theta\cos\theta & \sin^2\theta & 0 \\ 0 & 0 & 0 \end{bmatrix}, \tag{A2}$$

which leads to an expression for Eq. (16) that can be solved analytically; it being,

$$\boldsymbol{\kappa}(\varsigma) = \begin{bmatrix} \kappa_{11} & 0 & 0 \\ 0 & \kappa_{22} & 0 \\ 0 & 0 & 0 \end{bmatrix}, \tag{A3}$$

where the two non-zero stiffness components have values of

$$\kappa_{11} = \frac{1}{2} + \frac{e^{-2\varsigma^2}\left[\operatorname{erf}\left(\frac{\pi+i4\varsigma^2}{2\sqrt{2}\varsigma}\right) + \operatorname{erf}\left(\frac{\pi-i4\varsigma^2}{2\sqrt{2}\varsigma}\right)\right]}{4\operatorname{erf}\left(\frac{\pi}{2\sqrt{2}\varsigma}\right)}, \tag{A4}$$

and

$$\kappa_{22} = \frac{1}{2} - \frac{e^{-2\varsigma^2}\left[\operatorname{erf}\left(\frac{\pi+i4\varsigma^2}{2\sqrt{2}\varsigma}\right) + \operatorname{erf}\left(\frac{\pi-i4\varsigma^2}{2\sqrt{2}\varsigma}\right)\right]}{4\operatorname{erf}\left(\frac{\pi}{2\sqrt{2}\varsigma}\right)}, \tag{A5}$$

wherein $i = \sqrt{-1}$ is the unit imaginary number.

The sum of two error functions whose arguments are complex conjugates, i.e., $\operatorname{erf}(x + iy) + \operatorname{erf}(x - iy)$, produces a real result, and as such, κ_{11} and κ_{22} are both reals.

B Three-Dimensional Splay

Here the formulation is somewhat different; specifically,

$$\mathbf{a}_0 = \begin{Bmatrix} 1 \\ 0 \\ 0 \end{Bmatrix}, \quad \mathbf{e}_f = \begin{Bmatrix} \cos\theta \\ \sin\theta\cos\phi \\ \sin\theta\sin\phi \end{Bmatrix}, \tag{B1}$$

and as such

$$\mathbf{e}_f \otimes \mathbf{e}_f = \begin{bmatrix} \cos^2\theta & \sin\theta\cos\theta\cos\phi & \sin\theta\cos\theta\sin\phi \\ \sin\theta\cos\theta\cos\phi & \sin^2\theta\cos^2\phi & \sin^2\theta\sin\phi\cos\phi \\ \sin\theta\cos\theta\sin\phi & \sin^2\theta\sin\phi\cos\phi & \sin^2\theta\sin^2\phi \end{bmatrix}, \tag{B2}$$

which leads to an expression for Eq. (17) that can be solved analytically; it being,

$$\boldsymbol{\kappa}(\varsigma) = \begin{bmatrix} \kappa_{11} & 0 & 0 \\ 0 & \kappa_{22} & 0 \\ 0 & 0 & \kappa_{33} \end{bmatrix}, \tag{B3}$$

where the two non-zero stiffness components have values of

$$\kappa_{11} = \frac{1}{2} + \frac{e^{-2\varsigma^2}\left[\operatorname{erf}\left(\frac{\pi+i4\varsigma^2}{2\sqrt{2}\varsigma}\right) + \operatorname{erf}\left(\frac{\pi-i4\varsigma^2}{2\sqrt{2}\varsigma}\right)\right]}{4\operatorname{erf}\left(\frac{\pi}{2\sqrt{2}\varsigma}\right)}, \tag{B4}$$

which is the same as Eq. (A4), and

$$\kappa_{22} = \kappa_{33} = \frac{1}{4} - \frac{e^{-2\varsigma^2}\left[\operatorname{erf}\left(\frac{\pi+i4\varsigma^2}{2\sqrt{2}\varsigma}\right) + \operatorname{erf}\left(\frac{\pi-i4\varsigma^2}{2\sqrt{2}\varsigma}\right)\right]}{8\operatorname{erf}\left(\frac{\pi}{2\sqrt{2}\varsigma}\right)}, \tag{B5}$$

where this value for κ_{22} is exactly half that of Eq. (A5), wherein $\kappa_{33} = 0$, but here $\kappa_{33} = \kappa_{22}$.

Algorithm 1
Given H_0/r_0, R_0/r_0, E_f, and λ_u, where H_0 is the initial wavelength of crimp, R_0 is the initial amplitude of crimp, r_0 is the initial fibril radius, E_f is the elastic modulus of the fiber in the linear region, and λ_u is its ultimate stretch, then:

$$\text{Set} \quad r_0 = 1 \quad \text{so that} \quad H_0 \equiv H_0/r_0 \quad \& \quad R_0 \equiv R_0/r_0.$$

Compute the constant parameters:

$$L_0 = ((2\pi R_0)^2 + H_0^2)^{1/2}, \qquad \Lambda = L_0/H_0 < \lambda_u,$$
$$E_s = E_f/\{(H_0/L_0)^2 + [H_0(L_0 - H_0)/L_0^2][1 + 37/6\pi^2 + 2(L_0/\pi r_0)^2]\},$$

where L_0 is the chord length of helix over one wavelength, while Λ is the stretch and E_s is the secant modulus at the transition between the toe and linear regions.
If $\lambda \le \Lambda$ Then

$$\xi = 6(\pi r_0)^2[\Lambda^2 + (4\pi^2 - 1)\lambda^2]\lambda$$
$$/\ \{\Lambda\{3H_0^2(\Lambda^2 - \lambda^2)[3\Lambda^2 + (8\pi^2 - 3)\lambda^2] + 8(\pi r_0)^2[10\Lambda^2 + (3\pi^2 - 10)\lambda^2]\}\},$$
$$\begin{aligned} d\xi/d\lambda = \{&18H_0^2(\pi r_0)^2[3\Lambda^6 + (28\pi^2 - 3)\Lambda^4\lambda^2 + (32\pi^4 - 8\pi^2 - 3)\Lambda^2\lambda^4 \\ &+ (32\pi^4 - 20\pi^2 + 3)\lambda^6] + 48(\pi r_0)^4[10\Lambda^4 \\ &+ (117\pi^2 - 20)\Lambda^2\lambda^2 + (12\pi^4 - 43\pi^2 + 10)\lambda^4]\} \\ / \{&\Lambda\{3H_0^2(\Lambda^2 - \lambda^2)[3\Lambda^2 + (8\pi^2 - 3)\lambda^2] \\ &+ 8(\pi r_0)^2[10\Lambda^2 + (3\pi^2 - 10)\lambda^2]\}^2\}, \end{aligned}$$
$$\sigma/\lambda = E_s\xi(\lambda - 1)/\lambda^2 \quad \& \quad d\sigma/d\lambda = E_s[\xi/\lambda^2 + (d\xi/d\lambda)(\lambda - 1)/\lambda]$$

Else If $\Lambda \le \lambda \le \lambda_u$ Then

$$\sigma/\lambda = E_s(\Lambda - 1)/\Lambda\lambda + E_f(\lambda - \Lambda)/\lambda \quad \& \quad d\sigma/d\lambda = E_f$$

Else Fibril Failure

$$\sigma/\lambda = 0 \quad \& \quad d\sigma/d\lambda = 0.$$

Return σ/λ and $d\sigma/d\lambda$.

C Collagen Model

A micro-structural model based on the physiology of crimped collagen fibers was recently derived by [Freed and Doehring, 2004] that we have altered to meet our needs (see Alg. 1); specifically, given a fiber stretch λ, this model returns the true stress σ/λ and tangent modulus $d\sigma/d\lambda$ of the fiber. There are four physiologic parameters (material constants defined at the top of the algorithm) that the user must supply; three if failure is not to be considered.

A typical pair of response curves are plotted in Fig. 8. The discontinuity observed in the $d\sigma/d\lambda$ curve indicates that the model presented in Alg. 1 predicts a stress σ response that is continuous and once-differentiable in stretch λ up to fiber failure, which is not depicted in this figure. The values assigned to the model to obtain these curves were $H_0/r_0 = 27.5$, $R_0/r_0 = 2$, and $E_f = 45$MPa, which results in a transitional stretch of $\Lambda \approx 1.1$.

This is but one example of a fiber stress/stretch model.

D Voigt Notation

Because the Lagrangian fields for stress S_{ij} and strain E_{ij}, $i, j = 1, 2, 3$, are symmetric tensors, it is customary to express their components as six-dimensional arrays S_α and E_α, $\alpha = 1, 2, \ldots, 6$. These arrays are not vector fields in the sense that

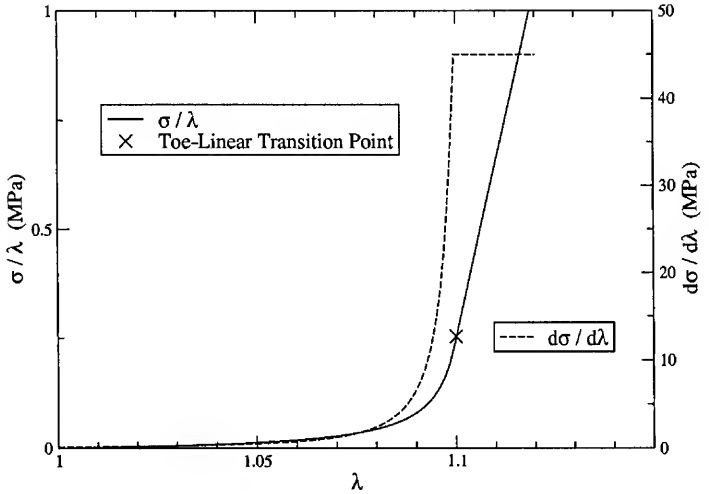

Figure 8 Typical soft-tissue response curves for σ/λ and $\mathrm{d}\sigma/\mathrm{d}\lambda$.

they do not obey the tensor-transformation law. Nevertheless, they have proven to be very useful in the employ of finite elements.

Given a Cartesian reference frame, the stress and strain arrays can be expressed in terms of their tensor components via[9]

$$S_\alpha = \begin{Bmatrix} S_1 \\ S_2 \\ S_3 \\ S_4 \\ S_5 \\ S_6 \end{Bmatrix} = \begin{Bmatrix} S_{11} \\ S_{22} \\ S_{33} \\ S_{12} = S_{21} \\ S_{13} = S_{31} \\ S_{23} = S_{32} \end{Bmatrix} \quad \text{and} \quad E_\alpha = \begin{Bmatrix} E_1 \\ E_2 \\ E_3 \\ E_4 \\ E_5 \\ E_6 \end{Bmatrix} = \begin{Bmatrix} E_{11} \\ E_{22} \\ E_{33} \\ E_{12} + E_{21} \\ E_{13} + E_{31} \\ E_{23} + E_{32} \end{Bmatrix}, \tag{D1}$$

which is commonly referred to as Voigt notation [Belytschko et al., 2000, pp. 615–618]. From thermodynamics, stress is described in terms of a potential function W through the gradient

$$S_{ij} = \varrho_0 \left(\frac{\partial W}{\partial C_{ij}} + \frac{\partial W}{\partial C_{ji}} \right) \quad \therefore \quad S_{ij} = S_{ji}, \tag{D2}$$

where C_{ij} is the Lagrangian (or Green) deformation field. It is more common to see the above formula written in the condensed notation of tensors $\mathbf{S} = 2\varrho_0 \partial W/\partial \mathbf{C}$ (see Eq. 8) with the implication being that its components are computed via Eq. (D2).

[9] A note of caution. Some implementations exchange S_4 and S_6, and likewise, E_4 and E_6. This has no effect on formulæ written using Voigt notation, provided that the components are correctly mapped between their tensor and Voigt representations.

A stress increment $\mathrm{d}S_{ij}$ is therefore related to a strain increment $\mathrm{d}E_{ij} = \frac{1}{2}\mathrm{d}C_{ij}$ in the Lagrangian frame through the linear approximation

$$\mathrm{d}S_{ij} = M_{ijk\ell}\mathrm{d}E_{k\ell} \quad \text{with} \quad M_{ijk\ell} = \frac{\partial S_{ij}}{\partial E_{k\ell}} \quad \therefore \quad \mathrm{d}S_{\alpha} = M_{\alpha\beta}\mathrm{d}E_{\beta}, \tag{D3}$$

where the tangent modulus $M_{ijk\ell}$ has a Voigt representation of

$$M_{\alpha\beta} = \begin{bmatrix} M_{11} & M_{12} & M_{13} & M_{14} & M_{15} & M_{16} \\ M_{21} & M_{22} & M_{23} & M_{24} & M_{25} & M_{26} \\ M_{31} & M_{32} & M_{33} & M_{34} & M_{35} & M_{36} \\ M_{41} & M_{42} & M_{43} & M_{44} & M_{45} & M_{46} \\ M_{51} & M_{52} & M_{53} & M_{54} & M_{55} & M_{56} \\ M_{61} & M_{62} & M_{63} & M_{64} & M_{65} & M_{66} \end{bmatrix} = \begin{bmatrix} M_{1111} & M_{1122} & M_{1133} & M_{1112} & M_{1113} & M_{1123} \\ M_{2211} & M_{2222} & M_{2233} & M_{2212} & M_{2213} & M_{2223} \\ M_{3311} & M_{3322} & M_{3333} & M_{3312} & M_{3313} & M_{3323} \\ M_{1211} & M_{1222} & M_{1233} & M_{1212} & M_{1213} & M_{1223} \\ M_{1311} & M_{1322} & M_{1333} & M_{1312} & M_{1313} & M_{1323} \\ M_{2311} & M_{2322} & M_{2333} & M_{2312} & M_{2313} & M_{2323} \end{bmatrix}, \tag{D4}$$

with $M_{\alpha\beta} \neq M_{\beta\alpha}$ unless the $M_{ijk\ell}$ possess major symmetry $M_{ijk\ell} = M_{k\ell ij}$. The tangent modulus always possesses minor symmetries $M_{ijk\ell} = M_{ij\ell k} = M_{jik\ell} = M_{ji\ell k}$ because of the inherent symmetries in S_{ij} and C_{ij}. Major symmetry follows automatically if stress S_{ij} is given by a potential function F such that $S_{ij} = \partial F/\partial E_{ij}$, as is the case in elasticity (see Eq. D2).

From Eqs. (D2 & D3), it follows that the components of $M_{ijk\ell}$ are obtained via

$$M_{ijk\ell} = \varrho_0\left(\frac{\partial^2 W}{\partial C_{ij}\partial C_{k\ell}} + \frac{\partial^2 W}{\partial C_{ij}\partial C_{\ell k}} + \frac{\partial^2 W}{\partial C_{ji}\partial C_{k\ell}} + \frac{\partial^2 W}{\partial C_{ji}\partial C_{\ell k}}\right), \tag{D5}$$

so that $M_{ijk\ell} = M_{ij\ell k} = M_{jik\ell} = M_{ji\ell k}$ and $M_{ijk\ell} = M_{k\ell ij}$. In tensor notation, the tangent modulus is usually defined as $\mathsf{M} = 4\varrho_0\partial^2 W/\partial\mathsf{C}\,\partial\mathsf{C}$ (see Eq. 34) with the implication being that its components are computed via Eq. (D5).

D.1 Tensor Products

Two tensor products naturally arise in constitutive construction that we denote as $\mathsf{A}\boxtimes\mathsf{B}$ and $\mathsf{A}\otimes\mathsf{B}$, and call the inner- and outer-dyadic products, respectively, or the circle- and box-products for short, wherein A and B are taken to be symmetric.

The box product $\mathsf{A}\boxtimes\mathsf{B}$ is defined by the sum

$$(A\boxtimes B)_{ijk\ell} = \tfrac{1}{4}(A_{ik}B_{j\ell} + A_{i\ell}B_{jk} + A_{jk}B_{i\ell} + A_{j\ell}B_{ik}), \tag{D6}$$

which possesses both minor and major symmetries, therefore $(A\boxtimes B)_{\alpha\beta} = (A\boxtimes B)_{\beta\alpha}$, and consequently, this product is commutative, i.e., $\mathsf{A}\boxtimes\mathsf{B} = \mathsf{B}\boxtimes\mathsf{A}$. The Voigt

representation of $(A \boxtimes B)_{\alpha\beta}$ has the symmetric matrix components:

$$\begin{cases}
(A \boxtimes B)_{11} = A_{11}B_{11}, \\
(A \boxtimes B)_{12} = A_{12}B_{12}, \\
(A \boxtimes B)_{13} = A_{13}B_{13}, \\
(A \boxtimes B)_{14} = \frac{1}{2}(A_{11}B_{12} + A_{12}B_{11}), \\
(A \boxtimes B)_{15} = \frac{1}{2}(A_{11}B_{13} + A_{13}B_{11}), \\
(A \boxtimes B)_{16} = \frac{1}{2}(A_{12}B_{13} + A_{13}B_{12}), \\
(A \boxtimes B)_{22} = A_{22}B_{22}, \\
(A \boxtimes B)_{23} = A_{23}B_{23}, \\
(A \boxtimes B)_{24} = \frac{1}{2}(A_{12}B_{22} + A_{22}B_{12}), \\
(A \boxtimes B)_{25} = \frac{1}{2}(A_{12}B_{23} + A_{23}B_{12}), \\
(A \boxtimes B)_{26} = \frac{1}{2}(A_{22}B_{23} + A_{23}B_{22}), \\
(A \boxtimes B)_{33} = A_{33}B_{33}, \\
(A \boxtimes B)_{34} = \frac{1}{2}(A_{13}B_{23} + A_{23}B_{13}), \\
(A \boxtimes B)_{35} = \frac{1}{2}(A_{13}B_{33} + A_{33}B_{13}), \\
(A \boxtimes B)_{36} = \frac{1}{2}(A_{23}B_{33} + A_{33}B_{23}), \\
(A \boxtimes B)_{44} = \frac{1}{4}(A_{11}B_{22} + 2A_{12}B_{12} + A_{22}B_{11}), \\
(A \boxtimes B)_{45} = \frac{1}{4}(A_{11}B_{23} + A_{13}B_{12} + A_{12}B_{13} + A_{23}B_{11}), \\
(A \boxtimes B)_{46} = \frac{1}{4}(A_{12}B_{23} + A_{13}B_{22} + A_{22}B_{13} + A_{23}B_{12}), \\
(A \boxtimes B)_{55} = \frac{1}{4}(A_{11}B_{33} + 2A_{13}B_{13} + A_{33}B_{11}), \\
(A \boxtimes B)_{56} = \frac{1}{4}(A_{12}B_{33} + A_{13}B_{23} + A_{23}B_{13} + A_{33}B_{12}), \\
(A \boxtimes B)_{66} = \frac{1}{4}(A_{22}B_{33} + 2A_{23}B_{23} + A_{33}B_{22}).
\end{cases} \tag{D7}$$

The circle product $\mathsf{A} \otimes \mathsf{B}$ has components

$$(A \otimes B)_{ijk\ell} = \tfrac{1}{4}(A_{ij}B_{k\ell} + A_{ij}B_{\ell k} + A_{ji}B_{k\ell} + A_{ji}B_{\ell k}) \equiv A_{ij}B_{k\ell}, \tag{D8}$$

which reduce down to the simple expression $(A \otimes B)_{ijk\ell} = A_{ij}B_{k\ell}$ as a consequence of A and B being symmetric. This well-known product has a Voigt notation of

$$(A \otimes B)_{\alpha\beta} = \begin{bmatrix}
A_{11}B_{11} & A_{11}B_{22} & A_{11}B_{33} & A_{11}B_{12} & A_{11}B_{13} & A_{11}B_{23} \\
A_{22}B_{11} & A_{22}B_{22} & A_{22}B_{33} & A_{22}B_{12} & A_{22}B_{13} & A_{22}B_{23} \\
A_{33}B_{11} & A_{33}B_{22} & A_{33}B_{33} & A_{33}B_{12} & A_{33}B_{13} & A_{33}B_{23} \\
A_{12}B_{11} & A_{12}B_{22} & A_{12}B_{33} & A_{12}B_{12} & A_{12}B_{13} & A_{12}B_{23} \\
A_{13}B_{11} & A_{13}B_{22} & A_{13}B_{33} & A_{13}B_{12} & A_{13}B_{13} & A_{13}B_{23} \\
A_{23}B_{11} & A_{23}B_{22} & A_{23}B_{33} & A_{23}B_{12} & A_{23}B_{13} & A_{23}B_{23}
\end{bmatrix}, \tag{D9}$$

where $(A \otimes B)_{\alpha\beta}$ is not symmetric unless $\mathsf{A} = \mathsf{B}$; however, $(\mathsf{A} \otimes \mathsf{B}) + (\mathsf{B} \otimes \mathsf{A})$ does yield a symmetric matrix in Voigt notation. This is because $\mathsf{A} \otimes \mathsf{B}$ possesses minor symmetry, but not major symmetry, in general. This dyadic product is not commutative.

D.2 Example

The theory of linear elasticity has stress components

$$\begin{cases} S_1 = S_{11} = \lambda(E_{11} + E_{22} + E_{33}) + 2\mu E_{11}, \\ S_2 = S_{22} = \lambda(E_{11} + E_{22} + E_{33}) + 2\mu E_{22}, \\ S_3 = S_{33} = \lambda(E_{11} + E_{22} + E_{33}) + 2\mu E_{33}, \\ S_4 = S_{12} = 2\mu E_{12}, \\ S_5 = S_{13} = 2\mu E_{13}, \\ S_6 = S_{23} = 2\mu E_{23}, \end{cases}$$

and as such, its tangent modulus is readily determined to be

$$M_{\alpha\beta} = \lambda(I \otimes I)_{\alpha\beta} + 2\mu(I \boxtimes I)_{\alpha\beta},$$

wherein λ and μ are the elastic moduli, and where

$$I_\alpha = \begin{Bmatrix} 1 \\ 1 \\ 1 \\ 0 \\ 0 \\ 0 \end{Bmatrix}, \quad (I \otimes I)_{\alpha\beta} = \begin{bmatrix} 1 & 1 & 1 & 0 & 0 & 0 \\ 1 & 1 & 1 & 0 & 0 & 0 \\ 1 & 1 & 1 & 0 & 0 & 0 \\ 0 & 0 & 0 & 0 & 0 & 0 \\ 0 & 0 & 0 & 0 & 0 & 0 \\ 0 & 0 & 0 & 0 & 0 & 0 \end{bmatrix}, \quad (I \boxtimes I)_{\alpha\beta} = \begin{bmatrix} 1 & 0 & 0 & 0 & 0 & 0 \\ 0 & 1 & 0 & 0 & 0 & 0 \\ 0 & 0 & 1 & 0 & 0 & 0 \\ 0 & 0 & 0 & \frac{1}{2} & 0 & 0 \\ 0 & 0 & 0 & 0 & \frac{1}{2} & 0 \\ 0 & 0 & 0 & 0 & 0 & \frac{1}{2} \end{bmatrix}.$$

The $\frac{1}{2}$'s in $(I \boxtimes I)_{\alpha\beta}$ are offset by the 2's present in $\mathrm{d}E_\beta$.

References

[Belytschko et al., 2000] Belytschko T, Liu WK, Moran B (2000) Nonlinear Finite Elements for Continua and Structures. John Wiley & Sons, Chichester

[Billiar and Sacks, 2000a] Billiar KL, Sacks MS (2000a) Biaxial mechanical properties of the natural and glutaraldehyde-treated aortic valve cusp—Part I: Experimental results. ASME J Biomech Eng, 122: 23–30

[Billiar and Sacks, 2000b] Billiar KL, Sacks MS (2000b) Biaxial mechanical properties of the natural and glutaraldehyde-treated aortic valve cusp—Part II: A structural constitutive model. ASME J Biomech Eng, 122: 327–335

[Cauchy, 1827] Cauchy AL (1827) Exercices de Mathématiques, vol 2. de Bure Frères, Paris

[Criscione et al., 2001] Criscione JC, Douglas AS, Hunter WC (2001) Physically based strain invariant set for materials exhibiting transversely isotropic behavior. J Mech Phys Solids, 49: 871–897

[Doehring et al., 2004] Doehring TC, Carew EO, Vesely I (2004) The effect of strain rate on the viscoelastic response of aortic valve tissue: A direct-fit approach. Ann Biomed Eng, 32: 223–232

[Einstein, 2002] Einstein DR (2002) Nonlinear Acoustic Analysis of the Mitral Valve. Ph.D. thesis, University of Washington, Seattle

[Finger, 1894] Finger J (1894) Über die allgemeinsten Beziehungen zwischen endlichen Deformationen und den zugehörigen Spannungen in aeolotropen und isotropen Substanzen. Sitzungsberichte der Akademie der Wissenschaften, Wien, 103: 1073–1100

[Flory, 1961] Flory PJ (1961) Thermodynamic relations for high elastic materials. Trans Faraday Soc, 57: 829–838

[Freed, 2004] Freed AD (2004) Transverse-isotropic elastic and viscoelastic solids. ASME J Eng Mater Technol, 126: 38–44

[Freed and Doehring, 2004] Freed AD, Doehring TC (2004) Elastic response of crimped collagen fibrils. ASME IMECE 2004/61578

[Green, 1841] Green G (1841) On the propagation of light in crystallized media. Trans Cambridge Phil Soc, 7: 121–140

[Hencky, 1928] Hencky H (1928) Über die Form des Elastizitätsgesetzes bei ideal elastischen Stoffen. Z tech Phys, 9: 215–220

[Holzapfel, 2000] Holzapfel GA (2000) Nonlinear Solid Mechanics: A continuum approach for engineering. John Wiley & Sons, Chichester

[Holzapfel et al., 2002] Holzapfel GA, Gasser TC, Stadler M (2002) A structural model for the viscoelastic behavior of arterial walls: Continuum formulation and finite element analysis. Eur J Mech A-Solids, 21: 441–463

[Horowitz et al., 1988] Horowitz A, Lanir Y, Yin FC, Perl M, Sheinman I, Strumpf RK (1988) Structural three-dimensional constitutive law for the passive myocardium. ASME J Biomech Eng, 110: 200–207

[Hurschler et al., 1997] Hurschler C, Loitz-Ramage B, Vanderby, Jr R (1997) A structurally based stress-stretch relationship for tendon and ligament. ASME J Biomech Eng, 119: 392–399

[Kaliske, 2000] Kaliske M (2000) A formulation of elasticity and viscoelasticity for fibre reinforced material at small and finite strains. Comp Meth Appl Mech Eng, 185: 225–243

[Lanir, 1983] Lanir Y (1983) Constitutive equations for fibrous connective tissues. J Biomech, 16: 1–12

[Leonov, 2000] Leonov AI (2000) On the conditions of potentiality in finite elasticity and hypo-elasticity. Int J Solids Struct, 37: 2565–2576

[Lodge, 1974] Lodge AS (1974) Body Tensor Fields in Continuum Mechanics: With applications to polymer rheology. Academic Press, New York

[Malkus and Hughes, 1978] Malkus DS, Hughes TJR (1978) Mixed finite element methods—Reduced and selective integration techniques: A unification of concepts. Comp Meth Appl Mech Eng, 15: 63–81

[Mijailovich et al., 1993] Mijailovich A, Stamenovic D, Fredberg JJ (1993) Toward a kinetic theory of connective tissue micromechanics. J Appl Physiol, 74: 665–681

[Mooney, 1940] Mooney M (1940) A theory of large elastic deformations. J Appl Phys, 11: 582–592

[Sacks, 2000] Sacks MS (2000) Biaxial mechanical evaluation of planar biological materials. J Elasticity, 61: 199–246

[Sacks, 2003] Sacks MS (2003) Incorporation of experimentally-derived fiber orientation into a structural consitutive model for planar collagenous tissues. ASME J Biomech Eng, 125: 280–287

[Simo and Hughes, 1998] Simo JC, Hughes TJR (1998) Computational Inelasticity, Interdisiplinary Applied Mathematics, vol 7. Springer-Verlag, New York

[Spencer, 1972] Spencer AJM (1972) Deformations of Fibre-reinforced Materials. Clarendon Press, Oxford

[Sussman and Bathe, 1987] Sussman T, Bathe KJ (1987) A finite element formulation for nonlinear incompressible elastic and inelastic analysis. Comput Struct, 26: 357–409

[Wuyts et al., 1995] Wuyts FL, Vanhuyse VJ, Langewouters GJ, Decraemer WF, Raman ER, Buyle S (1995) Elastic properties of human aortas in relation to age and atherosclerosis: A structural model. Phys Med Biol, 40: 1577–1597

[Zioupos and Barbenel, 1994] Zioupos P, Barbenel JC (1994) Mechanics of native bovine pericardium: I. The multiangular behavior of strength and stiffness of the tissue. Biomaterials, 15: 366–373